Isospecific Group Transfer Polymerization of Diethyl Vinylphosphonate and Multidimensional NMR Analysis of the Polymer Microstructure

Michael Weger,[1,‡] Philipp Pahl,[1,‡] Fabian Schmidt,[1,‡] Benedikt S. Soller,[1] Philipp J. Altmann,[2] Alexander Pöthig,[2] Gerd Gemmecker,[3] Wolfgang Eisenreich,[4,]* and Bernhard Rieger[1,]*

[1] Catalysis Research Center & WACKER-Chair of Macromolecular Chemistry, Technical University of Munich, Lichtenbergstraße 4, D-85747 Garching near Munich

[2] Catalysis Research Center & Chair of Inorganic and Metal-Organic Chemistry, Technical University of Munich, Lichtenbergstraße 4, D-85747 Garching near Munich

[3] Bavarian NMR Center, Technical University of Munich, Lichtenbergstraße 4, D-85747 Garching near Munich

[4] Chair of Biochemistry, Technical University of Munich, Lichtenbergstraße 4, D-85747 Garching near Munich

* Corresponding Author: rieger@tum.de, wolfgang.eisenreich@mytum.de

‡ These authors contributed equally.

1. Experimental Section 2

2. Single Crystal X-Ray Diffraction Experiments 11

3. Polymerization Studies and Mechanism Elucidation 20

4. NMR, GPC and Thermal Analysis of the PDEVP Samples 25

5. References 45

1. Experimental Section

Materials and Methods:

All reactions were carried out under argon atmosphere using standard Schlenk or glovebox techniques. All glassware was heat dried under vacuum prior to use. Unless otherwise stated, all chemicals were purchased from Sigma-Aldrich, VWR-International or ABCR and used as received. Toluene and tetrahydrofuran were dried using an MBraun SPS-800 solvent purification system. DEVP was dried over CaH_2 and destilled prior to use.

NMR spectra were recorded at 300 K on a Bruker AV-NEO 400 spectrometer equipped with a triple resonance TBI-probe, the $^{13}C\{^1H\}$ spectra on a Bruker AV-III-500 spectrometer equipped with a QNP-Cryoprobe and the $^1H\{^{31}P\}$ spectra on a Bruker AV-III-600 spectrometer equipped with a QCI-Cryoprobe. The details (acquisition parameters, pulse program) for the triple resonance experiments can be found in section 4. ^1H NMR spectroscopic chemical shifts δ are reported in ppm relative to tetramethylsilane. $\delta(^1H)$ is calibrated to the residual proton signal of the solvent. Deuterated solvents were obtained from Eurisotop or Sigma Aldrich.

For the ESI-MS analysis a Varian 500 LC MS ion trap spectrometer was used with acetonitrile as carrier (20 µl/min).

GPC was carried out on a Varian LC-920 equipped with two PL Polargel columns using tetrahydrofuran/water (1:1, 9 g/L tetrabutylammonium bromide) as eluent. Absolute molecular weights have been determined multiangle laser light scattering (MALLS) analysis (LC-920) using a Wyatt Dawn Heleos II in combination with a Wyatt Optilab rEX as concentration detector, coupled with GPC.

Elemental analysis was performed at the microanalytic laboratory of the Department of Inorganic Chemistry at the Technical University of Munich.

DSC measurements were carried out at a DSC G2000 of TA instruments with a heating rate of 1 °C/min in the first and 20 °C/min in the third cycle and a cooling rate of 5 °C/min.

Thermal gravimetric analysis (TGA) of the materials was carried out with a NETZSCH STA449 F5 Jupiter machine using aluminum oxide pans (70 µL with lid) with sample amounts of 1 to 5 mg. Temperature calibration of the oven cell was performed on the basis of the following metals: In, Sn, Bi, Zn, Al and Au. The baseline was corrected screening an empty sample pan with the respective measurement program prior to the experiment. The following thermal program was applied using argon gas (20 mL/min) for purging: At 27 °C isothermal equilibration (30 min), ramp from 27 °C to 800 °C with 10 K/min, isothermal equilibrium for 5 minutes.

General procedure for the polymerization of DEVP:

Polymerizations were performed in 30 mL oven-dried glass reactors interfaced to a dual-manifold Schlenk line at various temperatures under argon atmosphere. A predetermined amount of a catalyst was first dissolved in toluene. Then the polymerization was started by addition of the monomer (1 mL) *via* a gastight syringe under vigorous stirring. After the measured time interval, a 0.2 mL aliquot was taken from the reaction mixture *via* a syringe and quickly quenched into a 4 mL vial containing 0.4 mL of undried “wet” MeOD-d_4. The quenched aliquots were later analyzed by ^{1}H-NMR and ^{31}P-NMR to obtain the percent polymer yield data. The polymerization was immediately quenched after the removal of the aliquot by addition of 0.5 mL methanol. The solvents were evaporated from the quenched mixtures under reduced pressure, the polymers were purified by precipitation in pentane and dried in a vacuum oven at 50 °C overnight to a constant weight.

Activity measurements:

The stated amount of catalyst is dissolved in toluene and the reaction mixture is thermostated to the desired temperature. Then, the stated amount of monomer is added. During the course of the measurement, the temperature is monitored with a digital thermometer and aliquots (0.5 ml) are taken and quenched by addition to MeOD-d_4 (0.2 ml). After the stated reaction time, the reaction is quenched by addition of MeOH (0.5 ml). The procedure was performed at least twice for every polymerization to obtain accurate activity values The TOFs are calculated corresponding to the following equation:[1]

$$TOF = \frac{n(Mon)}{n(Cat) \times t} = \frac{n(Mon)_0 \times X}{n(Cat) \times t}$$

Characterization of Synthesized Organometallic Compounds:

The ligands $(C_5Me_4H)CH_2CH_2NH\textit{t}Bu$,[2] $(C_9H_7)SiMe_2NH\textit{t}Bu$,[3] $(C_5Me_4H)SiMe_2NHPh$[4] and $(C_5Me_4H)SiMe_2NH\textit{t}Bu$[5] were synthesized according to literature procedures.

$LiCH_2TMS$ 1.72 g Lithium granulate (249 mmol, 3.3 eq.) and 9.25 g chloromethyltrimethylsilane (75.0 mmol, 1 eq.) are suspended in 100 mL hexane and the mixture is heated at 35 °C for 24 h. Lithium is exempt of lithiumchloride several times using an ultrasonic bath. The supernatant solution is isolated using a filter cannula. The residue is extracted three times with hexane (15 ml) and the solvent is removed in vacuo, yielding a white pyrophoric solid (6.25 g, 66.0 mmol, 88%). ^{1}H NMR (400 MHz, C_6D_6) δ = 0.16 (s, 9H), -2.08 (s, 2H). ^{13}C NMR (126 MHz, C_6D_6) δ = 3.6, −4.7. elemental analysis calcd (%) for $C_4H_{11}LiSi$: C, 51.03; H, 11.78. Found: C, 51.14; H, 12.00.

$YCl_3(thf)_{3.5}$ A glass thimble is charged inside a glovebox to 2/3 with yttrium(III) chloride and is placed in a Soxhlet extractor. All glass joints of the reaction setup are diligently sealed using Teflon grease. The Soxhlet extractor is attached to a Schlenk flask with 150 mL THF, a reflux condenser, and a pressure valve using a Schlenk line outside the glovebox. The oil bath is heated at 110 °C and THF is heated to reflux for 36 h under vigorous stirring. After cooling the Schlenk flask to room temperature and detaching it from the reaction setup, THF is removed in vacuo. The product is obtained as a white powder and the amount of coordinating THF is determined by elemental analysis. The yield is nearly quantitative if pure yttrium (III)chloride is used as a starting material. Elemental analysis calcd. for $YCl_3(thf)_{3.5}$: C 37.56, H 6.30. Found: C 37.45, H 6.33.

$YCH_2TMS_3(thf)_2$ 1.79 g $YCl_3(thf)_{3.5}$ (4.00 mmol, 1 eq.) is suspended in 25 mL pentane. A solution of 1.13 g trimethylsilylmethyl lithium (12 mmol, 3 eq.) in 35 mL pentane is added dropwise at 0 °C and the reaction solution is stirred at 0 °C for 2 h. The supernatant solution is isolated using a filter cannula and the residue is extracted with pentane (2 × 10 mL). The solvent is removed in vacuo and the product is obtained as a white solid (1.78 g, 3.60 mmol, 90%). ^{1}H NMR (400 MHz, C_6D_6) δ = 4.01–3.87 (m, 8 H, THF-H), 1.36–1.21 (m, 8 H, THF-H), 0.31 (s, 27 H, CH_2SiMe_3), −0.67 (d, 6 H, CH_2SiMe_3). ^{13}C NMR (126 MHz, C_6D_6) δ = 69.8, 33.8, 25.2, 4.5.

$(C_5Me_4)Me_2SiN$*t*$BuYCH_2TMS(thf)$ was synthesized according to an literature procedure.[6] Recrystallization from pentane yields a colorless powder (2.29 g, 4.60 mmol, 52%). ^{1}H NMR (400 MHz, C_6D_6) δ = 3.38−3.15 (m, 4H, THF-H), 2.21 (s, 12H, CH_3), 1.39 (s, 9H, $NC(CH_3)_3$), 1.03−0.96 (m, 4H, THF-H), 0.77 (s, 6H, $SiMe_2$), 0.31 (s, 9H, CH_2SiMe_3), −0.90 (d, ^1J = 3.2 Hz, 2H, YCH_2). ^{13}C NMR (126 MHz, C_6D_6) δ = 126.4, 122.3, 106.6, 70.7, 54.0, 36.0, 26.2, 24.7, 14.0, 11.5, 8.4, 4.7. ^{29}Si NMR (99 MHz, C_6D_6) δ = −2.73, −25.06. Anal. Calcd for $C_{23}H_{46}NOSi_2Y$: C, 55.51; H, 9.32; N, 2.81. Found: C, 55.77; H, 9.50; N, 2.85.

$(C_5Me_4)CH_2CH_2N$*t*$BuYCH_2TMS(thf)$ 988 mg $Y(CH_2TMS)_3(thf)_2$ (1.89 mmol, 1 eq.) is dissolved in 18 mL pentane and the mixture is cooled to 0 °C. A solution of 418 mg $(C_5Me_4H)CH_2CH_2NH$*t*Bu (1.89 mmol, 1 eq.) in 7 mL pentane is added dropwise and the reaction solution is stirred for two hours at 0 °C. Volatile compounds are removed in vacuo, resulting in a yellow solid. The crude product is washed with cold pentane and dried in vacuo. The product is purified by recrystallization from pentane and is obtained as a slightly yellow crystalline solid (787 mg, 1.68 mmol, 89%). ^{1}H NMR (400 MHz, C_6D_6) δ = 3.89–3.81 (m, 2H, CH_2CH_2N), 3.60–3.20 (m, 4H, THF-H), 3.08 - 3.01 (t, 2H, CH_2CH_2N), 2.25–1.96 (m, 12H, CH_3), 1.34 (s, 9H, $NC(CH_3)_3$), 1.08–0.97 (m, 4H, THF-H), 0.36 (s, 9H, CH_2SiMe_3), -0.97 (d, 2H, YCH_2). ^{13}C NMR (126 MHz, C_6D_6) δ = 126.4, 126.2, 126.0, 68.5, 53.7, 52.4, 28.2, 25.8, 23.2, 22.7, 9.1, 3.0, -2.0. ^{29}Si NMR (99 MHz, C_6D_6) δ = -2.86. elemental analysis calcd (%) for $C_{23}H_{44}NOSiY$: C 59.08, H 9.48, N 3.00. Found: C 58.70, H 9.43, N 3.17.

$(C_5Me_4)Me_2SiNPhYCH_2TMS(thf)_2$ 959 mg $Y(CH_2TMS)_3(thf)_2$ (1.96 mmol, 1.1 eq.) is dissolved in 10 mL hexane and the mixture is cooled to 0 °C. A solution of 480 mg $(C_5Me_4H)SiMe_2NHPh$ (1.77 mmol, 1 eq.) in 5 mL hexane is added dropwise and the reaction solution is stirred for two hours at r.t. After filtration the residue is washed with pentane (2 × 5 mL) and dried in vacuo. The product is purified by diffusion crystallization in toluene/pentane at –35 °C and obtained as a colorless crystalline solid (870 mg, 1.49 mmol, 84%). ^{1}H NMR (400 MHz, C_6D_6) δ = 7.27-7.20 (m, 2H, Ph-H), 6.73-6.64 (m, 3H, Ph-H), 3.69−3.53 (m, 8H, THF-H), 2.11 (s, 6H, CH_3), 2.06 (s, 6H, CH_3), 1.42−1.31 (m, 8H, THF-H), 0.85 (s, 6H, $SiMe_2$), 0.25 (s, 9H, CH_2SiMe_3), −1.07 (d, ^{1}J = 2.6 Hz, 2H, YCH_2). ^{13}C NMR (126 MHz, C_6D_6) δ = 156.6, 129.4, 126.8, 122.6, 119.6, 114.5, 105.6, 68.2, 25.3, 21.4, 13.7, 11.4, 4.7, 4.3. ^{29}Si NMR (99 MHz, C_6D_6) δ = −2.44, −23.69. elemental analysis calcd (%) for $C_{29}H_{50}NO_2Si_2Y$: C, 59.06; H, 8.55; N, 2.37. Found: C, 58.75; H, 8.25; N, 2.29.

$(C_9H_6)Me_2SiN\mathit{t}BuYCH_2TMS(thf)$ 2.10 g $Y(CH_2TMS)_3(thf)_2$ (4.24 mmol, 1. eq.) is dissolved in 50 mL pentane and the mixture is cooled to 0 °C. A solution of 1.04 mg $(C_9H_7)SiMe_2NH\mathit{t}Bu$ (4.24 mmol, 1 eq.) in 8 mL pentane is added dropwise and the reaction solution is stirred over night at r.t. After filtration the filtrate is reduced to 10 mL and the product precipitates at –78 °C as a colorless crystalline solid (470 mg, 960 µmol, 23%). After drying the solid in vacuo, the known instability can be observed.[7] ^{1}H NMR (400 MHz, C_6D_6) δ = 7.89-7.81 (m, 1H, H_{Ind}), 7.54 – 7.46 (m, 1H, H_{Ind}), 7.15 – 7.12 (m, 1H, H_{Ind}), 7.06 –7.01 (m, 1H, H_{Ind}), 6.79-6.70 (m, 2H, H_{Ind}), 2.95−2.82 (m, 4H, THF-H), 1.30 (s, 9H, $NC(CH_3)_3$), 0.91 (s, 3H, $SiMe_2$), 0.88−0.82 (m, 4H, THF-H), 0.80 (s, 3H, $SiMe_2$), 0.38 (s, 9H, CH_2SiMe_3), −0.79 (dd, ^{1}J = 3.5 Hz, 1H, YCH_2), −0.97 (dd, ^{1}J = 3.5 Hz, 1H, YCH_2). ^{13}C NMR (126 MHz, C_6D_6) δ = 134.4, 131.8, 128.0, 123.4, 122.1, 120.8, 120.7, 104.2, 100.0, 70.3, 53.5, 35.5, 29.8, 24.3, 5.9, 4.3, 4.0. ^{29}Si NMR (99 MHz, C_6D_6) δ = −3.36, −24.34.

$(C_5Me_4)SiMe_2N$*t*BuY(2,6-lutidinyl) (1) 2.20 g $(C_5Me_4)SiMe_2N$*t*$BuYCH_2TMS$(thf) (4.40 mmol, 1 eq.) is dissolved in 100 mL pentane and 472 mg 2,6-lutidine (4.4 mmol, 1 eq.) in 20 mL pentane are added dropwise to the stirred solution. The mixture is stirred at room temperature for 30 minutes and volatile compounds are removed in vacuo. The residue is washed once with cold pentane and recrystallization from a saturated toluene-solution yields yellow crystals (1.78 g, 4.0 mmol, 91%). ^{1}H NMR (400 MHz, C_6D_6) $\delta = 6.76$ (dd, $^3J = 8.1$ Hz, $^3J = 7.7$ Hz, 1H, H_{ar}), 6.46 (d, $^3J = 8.1$ Hz, 1H, H_{ar}), 5.98 (d, $^3J = 7.7$ Hz, 1H, H_{ar}), 2.52 (s, 3H, $C\mathit{H}_3$), 2.33 (s, 3H, $C\mathit{H}_3$), 2.15 (s, 3H, $C\mathit{H}_3$), 2.02 (s, 3H, $C\mathit{H}_3$), 1.85 (s, 3H, $C\mathit{H}_3$), 1.41 (s, 2H, $YC\mathit{H}_2$), 1.00 (s, 9H, $NC(C\mathit{H}_3)_3$), 0.83 (s, 3H, $SiMe_2$), 0.74 (s, 3H, $SiMe_2$). ^{13}C NMR (126 MHz, C_6D_6) $\delta = 172.2$, 155.0, 138.7, 127.2, 126.6, 122.8, 122.0, 114.3, 106.7, 54.4, 41.3, 33.7, 26.0, 15.6, 14.1, 11.4, 11.0, 8.3, 7.4. ^{29}Si NMR (99 MHz, C_6D_6) $\delta = -25.37$. elemental analysis calcd (%) for $C_{22}H_{35}N_2SiY$: C, 59.44; H, 7.94; N, 6.30. Found: C, 59.66; H, 8.20; N, 6.22.

$(C_5Me_4)CH_2CH_2N$*t*BuY(2,6-lutidinyl) (2) 20.0 mg $(C_5Me_4)CH_2CH_2N$*t*$BuYCH_2TMS$(thf) (42.8 μmol, 1 eq.) is dissolved in 0.6 mL C_6D_6 and 4.58 mg 2,6-lutidine (42.8 μmol, 1 eq.) are added dropwise to the stirred solution. The mixture is stirred at room temperature for 30 minutes and NMR analysis shows quantitative conversion. ^{1}H NMR (400 MHz, C_6D_6) $\delta = 6.79$-6.72 (m, 1H, H_{ar}), 6.45-6.39 (m, 1H, H_{ar}), 6.01 (d, 1H, H_{ar}), 3.61-3.57 (m, 2H, $CH_2C\mathit{H}_2N$), 3.11-3.06 (m, 2H, $C\mathit{H}_2CH_2N$), 2.45 (s, 3H, $C\mathit{H}_3$), 2.35 (s, 2H, $YC\mathit{H}_2$), 2.34 (s, 3H, $C\mathit{H}_3$), 2.20 (s, 3H, $C\mathit{H}_3$), 2.01 (s, 3H, $C\mathit{H}_3$), 1.11 (s, 9H, $NC(C\mathit{H}_3)_3$).

$(C_9H_6)SiMe_2N$*t*BuY(2,6-lutidinyl) (3) 20.0 mg $(C_9H_6)SiMe_2N$*t*$BuYCH_2TMS$(thf) (39.5 μmol, 1 eq.) is dissolved in 0.6 mL C_6D_6 and 4.23 mg 2,6-lutidine (39.5 μmol, 1 eq.) are added dropwise to the stirred solution. The mixture is stirred at room temperature for 30 minutes and NMR analysis shows quantitative conversion. Diffusion crystallization in C_6D_6/pentane at –30 °C yields yellow crystals. ^{1}H NMR (400 MHz, C_6D_6) $\delta = 8.08$-8.03 (m, 1H, H_{Ind}), 7.54–7.49 (m, 1H, H_{Ind}), 7.09-7.03 (m, 1H, H_{Ind}), 6.82-6.67 (m, 4H, H_{Ind}, H_{ar}), 6.18-6.14 (m, 1H, H_{ar}), 6.07-6.01 (m, 1H, H_{ar}), 2.41 (s, 6H, $C\mathit{H}_3$), 1.15 (s, 9H, $NC(C\mathit{H}_3)_3$), 1.00 (s, 3H, $SiMe_2$), 0.88 (s, 3H, $SiMe_2$), 0.29 (s, 2H, $YC\mathit{H}_2$). ^{13}C NMR (126 MHz, C_6D_6) $\delta = 169.0$, 164.7, 156.3, 136.3, 133.6, 131.6, 126.5, 124.4, 122.0, 120.6, 120.1, 115.7, 104.0, 54.2, 43.1, 34.5, 24.7, 6.4, 4.3. ^{29}Si NMR (99 MHz, C_6D_6) $\delta = -24.65$. elemental analysis calcd (%) for C22H29YN2Si: C, 60.26; H, 6.67; N, 6.39. Found: C, 59.92; H, 7.04; N, 7.09.

$(C_5Me_4)SiMe_2NPhY$(2,6-lutidinyl) (4) 20.0 mg $(C_5Me_4)Me_2SiNPhYCH_2TMS(thf)_2$ (33.9 μmol, 1 eq.) is dissolved in 0.6 mL C_6D_6 and 3.63 mg 2,6-lutidine (33.9 μmol, 1 eq.) are added dropwise to the stirred solution. The mixture is stirred at room temperature for 30 minutes and NMR analysis shows quantitative conversion. ^{1}H NMR (400 MHz, C_6D_6) δ = 7.29-7.17 (m, 2H, Ph-H), 6.72 (t, 2H, Ph-H), 6.55 (d, 1H, Ph-H), 6.38 (s, 1H, H_{ar}), 6.29-6.22 (m, 1H, H_{ar}), 5.69 (s, 1H, H_{ar}), 2.17 (s, 6H, CH_3), 2.12 (s, 3H, CH_3), 2.10 (s, 2H, YCH_2), 2.04 (s, 3H, CH_3), 1.87 (s, 3H, CH_3), 0.97 (s, 6H, $SiMe_2$). ^{13}C NMR (126 MHz, C_6D_6) δ = 165.9, 156.5, 155.4, 147.1, 137.5, 129.2, 129.0, 128.2, 126.7, 125.3, 123.0, 119.4, 115.7, 115.2, 110.9, 106.9, 48.3, 31.6, 22.9, 14.0, 13.5, 11.1, 4.5. ^{29}Si NMR (99 MHz, C_6D_6) δ = −22.49.

$(C_5Me_4)CH_2CH_2N$*t*BuMg · 2 THF 5.00 g $(C_5Me_4H)CH_2CH_2NH$*t*Bu (22.6 mmol, 1.0 eq.) are dissolved in 100 ml toluene and 5 mL THF. The solution is cooled to 0 °C and 23.0 mL Di-*n*butylmagnesium (1.0 M in heptane, 3.14 g, 23.0 mmol, 1.0 eq.) is added within 30 minutes. After stirring the solution over night at r.t. the solvents are evaporated under high vacuum at 60 °C. Crystallization at –80 °C in THF yields a green solid (4.31 g, 17.7 mmol, 78%). ^{1}H NMR (400 MHz, C_6D_6) δ = 3.54 (m, 8H, THF-H), 3.15 (m, 1H, CH_2CH_2N), 2.70 (m, 1H, CH_2CH_2N), 2.65 (m, 1H, CH_2CH_2N), 2.48 (m, 1H, CH_2CH_2N), 2.24 (s, 3H, CH_3), 2.12 (s, 3H, CH_3), 2.06 (s, 3H, CH_3), 2.04 (s, 3H, CH_3), 1.33 – 1.49 (m, 8H, THF-H), 0.88 (s, 9H, $NC(CH_3)_3$). ^{13}C NMR (126 MHz, C_6D_6) δ = 116.2, 111.9, 110.9, 109.7, 106.7, 68.3, 52.2, 50.3, 34.1, 30.1, 25.7, 13.0, 12.2, 11.4, 11.1.

$(C_5Me_4)SiMe_2N$*t*BuMg · 2 THF 4.00 g $(C_5Me_4H)SiMe_2NH$*t*Bu (15.9 mmol, 1.0 eq.) are dissolved in 100 ml toluene and 5 mL THF. The solution is cooled to 0 °C and 16.2 mL Di-*n*butylmagnesium (1.0 M in heptane, 2.25 g, 16.2 mmol, 1.0 eq.) is added within 30 minutes. After stirring the solution over night at r.t. the solvents are evaporated under high vacuum at 60 °C. Crystallization at –80 °C in THF yields an orange solid (3.86 g, 11.2 mmol, 70%). ^{1}H NMR (400 MHz, C_6D_6) δ = 3.25 – 3.48 (m, 8H, THF-H), 2.52 (s, 6H, CH_3), 2.19 (s, 6H, CH_3), 1.42 (s, 9H, $NC(CH_3)_3$), 1.17 – 1.29 (m, 8H, THF-H), 0.98 (s, 6H, $SiMe_2$). ^{13}C NMR (126 MHz, C_6D_6) δ = 116.0, 114.2, 108.4, 69.1, 50.8, 37.6, 24.8, 14.7, 12.0, 8.6.

$(C_9H_6)SiMe_2N$*t*BuMg · 2 THF 5.00 g $(C_9H_7)SiMe_2NH$*t*Bu (20.4 mmol, 1.0 eq.) are dissolved in 60 ml toluene and 5 mL THF. The solution is cooled to 0 °C and 21.4 mL Di-*n*butylmagnesium (1.0 M in heptane, 2.96 g, 21.4 mmol, 1.0 eq.) is added within 30 minutes. After stirring the solution over night at r.t. the solvents are evaporated under high vacuum at 60 °C. Crystallization at –80 °C in THF yields a yellowish solid (4.38 g, 16.4 mmol, 70%). ^{1}H NMR (400 MHz, C_6D_6) δ = 8.18 (d, ^{3}J = 7.9 Hz, 1H, H_{ar}), 8.01 (d, ^{3}J = 7.9 Hz, 1H, H_{ar}), 7.31 (d, ^{3}J = 3.4 Hz, 1H, H_{ar}), 7.14 (dd, ^{3}J = 7.9 Hz, ^{3}J = 6.7 Hz, 1H, H_{ar}), 7.07 (dd, ^{3}J = 7.9 Hz, ^{3}J = 6.7 Hz, 1H, H_{ar}), 6.89 (d, ^{3}J = 3.5 Hz, 1H, H_{ar}), 3.15 (s, 8H, THF-H), 1.46 (s, 9H, $NC(CH_3)_3$), 1.12 (s, 8H, THF-H), 1.04 (s, 3H, SiMe$_2$), 0.91 (s, 3H, SiMe$_2$). ^{13}C NMR (126 MHz, C_6D_6) δ = 135.9, 135.1, 124.1, 120.8, 120.5, 116.7, 116.1, 103.5, 95.4, 69.7, 51.1., 38.1, 25.1, 6.6, 6.2.

(2,6-lutidinyl))AlCl$_2$ · THF 10.8 mL 2,6-lutidine (10.0 g, 93.3 mmol, 1.0 eq.) are dissolved in 100 mL THF and cooled to −78 °C. After slow addition of 39.2 mL *n*BuLi (2.5 M in pentane, 6.28 g, 1.05 eq.) a solution of 12.4 g aluminumchlorid (93.3 mmol, 1.0 eq.) in 300 mL THF is added within an hour. The mixture is carefully allowed to heat up to r.t. and the solvents are evaporated under reduced pressure. The residue is washed with 200 mL pentane and is suspended in 400 mL toluene after drying. The solvent of the filtrate is removed under vacuum. Crystallization at –90 °C in THF yields an off-white solid (18.8 g, 68.1 mmol, 73%). ^{1}H NMR (400 MHz, C_6D_6) δ = 6.91 (dd, ^3J = 7.6 Hz, ^3J = 7.7 Hz, 1H, H$_{ar}$), 6.76 (d, ^3J = 7.7 Hz, 1H, H$_{ar}$), 6.32 (d, ^3J = 7.6 Hz, 1H, H$_{ar}$), 3.78 – 3.91 (m, 4H, THF-H), 2.58 (s, 3H, CH_3), 1.97 (s, 2H, AlCH_2), 1.13 – 1.25 (m, 4H, THF-H). ^{13}C NMR (126 MHz, C_6D_6) δ = 164.2, 155.1, 139.2, 121.7, 121.3, 70.4, 25.1, 21.0, 16.3. ^{27}Al NMR (78 MHz, C_6D_6) δ = 81.5.

(C$_5$Me$_4$)SiMe$_2$N*t*BuAl(2,6-lutidinyl) (5) 5.62 g (C$_5$Me$_4$)SiMe$_2$N*t*BuMg · 2 THF (16.3 mmol, 1.0 eq.) are dissolved in 150 mL THF and cooled to −10 °C. A solution of 4.49 g (2,6-lutidinyl))AlCl$_2$ · THF (16.3 mmol, 1.0 eq.) in 20 mL THF is added within an hour. The mixture is stirred over night at r.t. and the solvent is evaporated under reduced pressure. The residue is suspended in 200 mL pentane and the solvent of the filtrate is removed. Orange crystals could be received by recrystallization in pentane at −60 °C (5.14 g, 13.4 mmol, 83%). ^{1}H NMR (400 MHz, C_6D_6) δ = 6.67 (dd, ^3J = 7.7 Hz, ^3J = 7.7 Hz, 1H, H$_{ar}$), 6.50 (d, ^3J = 7.7 Hz, 1H, H$_{ar}$), 6.15 (d, ^3J = 7.7 Hz, 1H, H$_{ar}$), 2.40 (s, 6H, CH_3), 2.21 (s, 3H, CH_3), 2.14 – 1.70 (m, 6H, CH_3), 1.32 – 1.59 (m, 2H, AlCH_2), 1.25 (s, 9H, NC(CH_3)$_3$), 0.81 (s, 6H, SiMe$_2$). ^{13}C NMR (126 MHz, C_6D_6) δ = 168.4, 154.3, 139.7, 122.7, 121.0, 108.3, 51.4, 35.7, 22.8, 19.1, 15.3, 11.6, 6.6. ^{27}Al NMR (78 MHz, C_6D_6) δ = 65.1. ^{29}Si NMR (60 MHz, C_6D_6) δ = −14.6. elemental analysis calcd (%) for C22H35AlN2Si: C, 69.06; H, 9.22; N, 7.32. Found: C, 69.28; H, 9.37; N, 7.10.

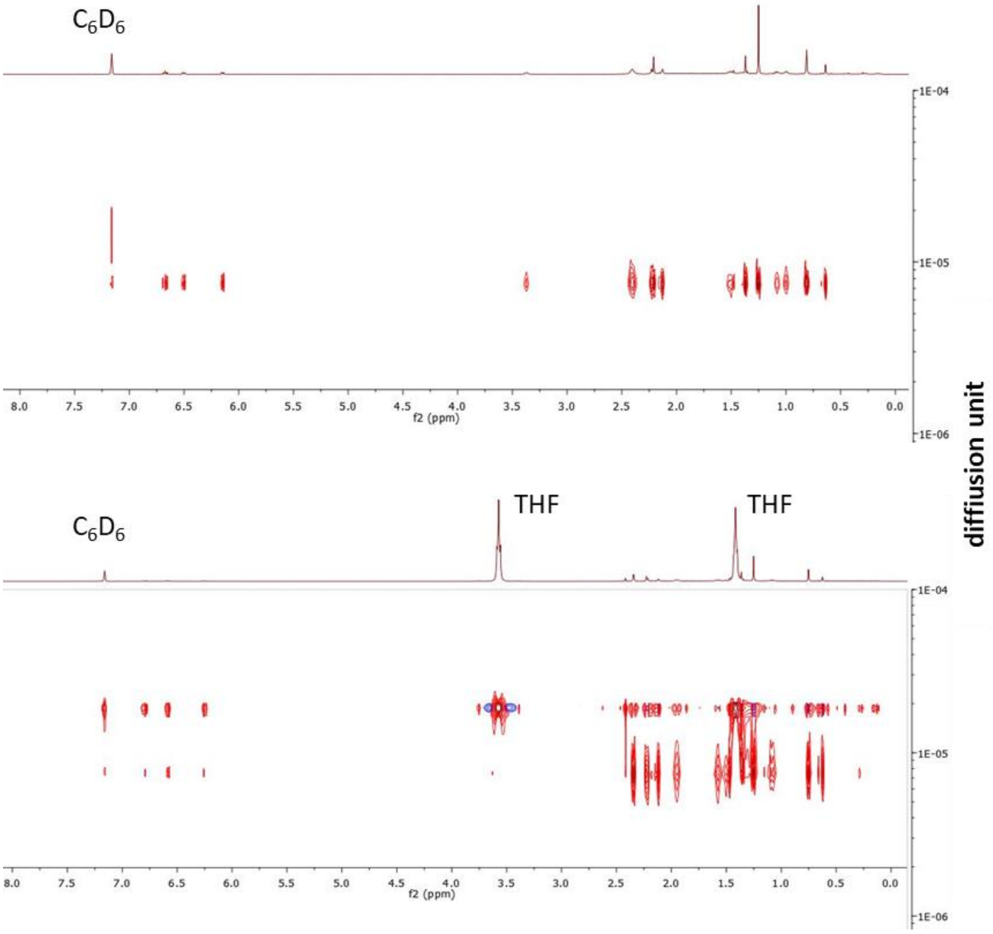

Figure S1. ^{1}H DOSY NMR spectra of **5** in C_6D_6 without (top) and with 10 eq. THF (bottom).

$(C_5Me_4)CH_2CH_2N$*t*BuAl(2,6-lutidinyl) (6) 1.25 g $(C_5Me_4)CH_2CH_2N$*t*BuMg · 2 THF (5.13 mmol, 1.0 Äq.) are dissolved in 50 mL THF and cooled to 0 °C. A solution of 1.42 g (2,6-lutidinyl))$AlCl_2$ · THF (5.13 mmol, 1.0 eq.) in 20 mL THF is added within 30 minutes. The mixture is stirred over night at r.t. and the solvent is evaporated under reduced pressure. The residue is suspended in 50 mL pentane and the solvent of the filtrate is removed. The red-brown solid could be received by precipitation in pentane −60 °C (1.02 g, 2.89 mmol, 56%). ^{1}H NMR (400 MHz, C_6D_6) $\delta = 6.73$ (dd, $^3J = 7.5$ Hz, $^3J = 7.6$ Hz, 1H, H_{ar}), 6.60 (d, $^3J = 7.6$ Hz, 1H, H_{ar}), 6.20 (d, $^3J = 7.5$ Hz, 1H, H_{ar}), 3.46 (t, $^3J = 6.6$ Hz, 2H, CH_2CH_2N), 3.05 (t, $^3J = 6.6$ Hz, 2H, CH_2CH_2N), 2.21 (s, 3H, CH_3), 2.16 (s, 6H, CH_3),2.14 – 1.88 (m, 6H, CH_3), 1.40 (s, 2H, $AlCH_2$), 1.15 (s, 9H, $NC(CH_3)_3$). ^{13}C NMR (126 MHz, C_6D_6) δ = 168.3, 153.7, 139.1, 129.3, 124.9, 122.6, 120.8, 105.6, 51.7, 45.0, 31.1, 27.1, 22.6, 11.9, 11.8, 11.2.

$(C_9H_6)SiMe_2N$*t*BuAl(2,6-lutidinyl) (7) 3.00 g $(C_9H_6)SiMe_2N$*t*BuMg · 2 THF (11.2 mmol, 1.0 Äq.) are dissolved in 150 mL toluene and cooled to 0 °C. A solution of 3.09 g (2,6-lutidinyl))$AlCl_2$ · THF (11.2 mmol, 1.0 eq.) in 50 mL toluene is added within an hour. The mixture is stirred over night at r.t. and the solvent is evaporated under reduced pressure. The residue is dissolved in 50 mL pentane and after one week at −45 °C, the solid is separated and dried. Yellow crystals could be received by recrystallization in toluene at −45 °C (3.29 g, 8.74 mmol, 78%). ^{1}H NMR (400 MHz, C_6D_6) δ = 7.62 (d, 1H, H_{Ind}), 7.09 – 7.16 (m, 1H, H_{Ind}), 6.82 – 6.88 (m, 2H, H_{Ind}), 6.67 – 6.76 (m, 2H, H_{ar}), 6.49 (d, ^3J = 4.7 Hz, 1H, H_{Ind}), 6.37 (d, ^3J = 4.7 Hz, 1H, H_{Ind}), 6.18 (d, 1H, H_{ar}), 2.86 (s, 6H, CH_3), 1.31 (s, 9H, $NC(CH_3)_3$), 1.28 (d, ^2J = 12.0 Hz, 1H, $AlCH_2$), 0.43 (s, 3H, $SiMe_2$), 0.33 (s, 3H, $SiMe_2$), 1.04 (d, ^2J = 12.0 Hz, 1H, $AlCH_2$). ^{13}C NMR (126 MHz, C_6D_6) δ = 169.2, 155.1, 146.1, 143.0, 138.7, 136.8, 122.9, 120.9, 120.6, 120.4, 120.3, 119.0, 116.3, 110.4, 51.3, 35.5, 28.3, 24.7, 6.6, 4.6. elemental analysis calcd (%) for C22H29AlN2Si: C, 70.17; H, 7.76; N, 7.44. Found: C, 69.92; H, 8.04; N, 7.09.

2. Single Crystal X-Ray Diffraction Experiments

SC-XRD determination of compound 1 (CCDC 1936317)

A yellow fragment-like specimen of $C_{26}H_{43}N_2OSiY$, approximate dimensions 0.139 mm x 0.148 mm x 0.156 mm, was used for the X-ray crystallographic analysis. The X-ray intensity data were measured on a Bruker D8 Venture system equipped with a Helios optic monochromator and a Mo TXS rotating anode ($\lambda = 0.71073$ Å).

A total of 1713 frames were collected. The total exposure time was 4.31 hours. The frames were integrated with the Bruker SAINT software package using a narrow-frame algorithm. The integration of the data using a monoclinic unit cell yielded a total of 60076 reflections to a maximum θ angle of 25.35° (0.83 Å resolution), of which 4876 were independent (average redundancy 12.321, completeness = 100.0%, R_{int} = 6.84%, R_{sig} = 2.79%) and 3942 (80.84%) were greater than $2\sigma(F^2)$. The final cell constants of $\underline{a}$ = 10.9805(4) Å, $\underline{b}$ = 20.9144(8) Å, $\underline{c}$ = 11.6587(4) Å, β = 94.721(2)°, volume = 2668.34(17) Å^3, are based upon the refinement of the XYZ-centroids of 132 reflections above 20 $\sigma(I)$ with $4.202° < 2\theta < 34.37°$. Data were corrected for absorption effects using the Multi-Scan method (SADABS). The ratio of minimum to maximum apparent transmission was 0.866. The calculated minimum and maximum transmission coefficients (based on crystal size) are 0.7200 and 0.7450.

The final anisotropic full-matrix least-squares refinement on F^2 with 290 variables converged at R1 = 3.34%, for the observed data and wR2 = 8.15% for all data. The goodness-of-fit was 1.070. The largest peak in the final difference electron density synthesis was 0.712 e$^-$/Å^3 and the largest hole was -0.613 e$^-$/Å^3 with an RMS deviation of 0.070 e$^-$/Å^3. On the basis of the final model, the calculated density was 1.286 g/cm^3 and F(000), 1096 e$^-$.

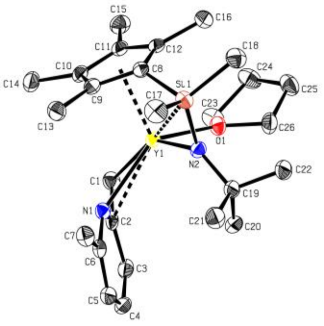

Figure S2. Ortep drawing with 50% ellipsoids for compound **1**.

Table S1. Sample and crystal data for compound **1**.

Identification code	PahPh7 AP9248-100	
Chemical formula	$C_{26}H_{43}N_2OSiY$	
Formula weight	516.62	
Temperature	100(2) K	
Wavelength	0.71073 Å	
Crystal size	0.139 x 0.148 x 0.156 mm	
Crystal habit	yellow fragment	
Crystal system	monoclinic	
Space group	P 1 21/n 1	
Unit cell dimensions	a = 10.9805(4) Å	$\alpha = 90°$
	b = 20.9144(8) Å	$\beta = 94.721(2)°$
	c = 11.6587(4) Å	$\gamma = 90°$
Volume	2668.34(17) Å^3	
Z	4	
Density (calculated)	1.286 g/cm^3	
Absorption coefficient	2.250 mm^{-1}	
F(000)	1096	

Table S2. Data collection and structure refinement for compound **1**.

Diffractometer	Bruker D8 Venture	
Radiation source	TXS rotating anode, Mo	
Theta range for data collection	1.95 to 25.35°	
Index ranges	-13<=h<=13, -25<=k<=25, -14<=l<=14	
Reflections collected	60076	
Independent reflections	4876 [R(int) = 0.0684]	
Coverage of independent reflections	100.0%	
Absorption correction	Multi-Scan	
Max. and min. transmission	0.7450 and 0.7200	
Refinement method	Full-matrix least-squares on F^2	
Refinement program	SHELXL-2014/7 (Sheldrick, 2014)	
Function minimized	$\Sigma\, w(F_o^2 - F_c^2)^2$	
Data / restraints / parameters	4876 / 0 / 290	
Goodness-of-fit on F^2	1.070	
Δ/σ_{max}	0.001	
Final R indices	3942 data; $I>2\sigma(I)$	R1 = 0.0334, wR2 = 0.0714
	all data	R1 = 0.0523, wR2 = 0.0815
Weighting scheme	$w=1/[\sigma^2(F_o^2)+(0.0234P)^2+4.9294P]$ where $P=(F_o^2+2F_c^2)/3$	

Largest diff. peak and hole	0.712 and -0.613 eÅ^{-3}
R.M.S. deviation from mean	0.070 eÅ^{-3}

SC-XRD determination of compound 3 (CCDC 1936316)

A clear colourless fragment-like specimen of $C_{22}H_{29}N_2SiY$, approximate dimensions 0.126 mm x 0.178 mm x 0.234 mm, was used for the X-ray crystallographic analysis. The X-ray intensity data were measured on a Bruker D8 Venture Duo IMS system equipped with a Helios optic monochromator and a Mo IMS microsource (λ = 0.71073 Å).

A total of 1563 frames were collected. The total exposure time was 0.82 hours. The frames were integrated with the Bruker SAINT software package using a narrow-frame algorithm. The integration of the data using a monoclinic unit cell yielded a total of 66552 reflections to a maximum θ angle of 29.57° (0.72 Å resolution), of which 5978 were independent (average redundancy 11.133, completeness = 100.0%, R_{int} = 9.34%, R_{sig} = 4.29%) and 4877 (81.58%) were greater than $2\sigma(F^2)$. The final cell constants of a = 10.4940(5) Å, b = 12.6978(6) Å, c = 15.9846(7) Å, β = 91.044(2)°, volume = 2129.61(17) Å^3, are based upon the refinement of the XYZ-centroids of 9863 reflections above 20 σ(I) with 4.682° < 2θ < 61.07°. Data were corrected for absorption effects using the Multi-Scan method (SADABS). The ratio of minimum to maximum apparent transmission was 0.793. The calculated minimum and maximum transmission coefficients (based on crystal size) are 0.5600 and 0.7190.

The final anisotropic full-matrix least-squares refinement on F^2 with 249 variables converged at R1 = 3.48%, for the observed data and wR2 = 6.92% for all data. The goodness-of-fit was 1.041. The largest peak in the final difference electron density synthesis was 0.461 e$^-$/Å^3 and the largest hole was -0.386 e$^-$/Å^3 with an RMS deviation of 0.084 e$^-$/Å^3. On the basis of the final model, the calculated density was 1.368 g/cm^3 and F(000), 912 e$^-$.

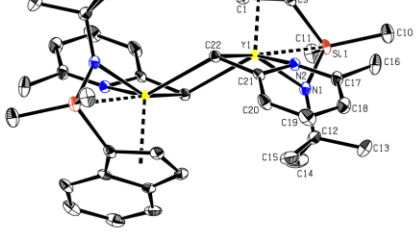

Figure S3. Ortep drawing with 50% ellipsoids for compound **3**.

Table S3. Sample and crystal data for compound **3**.

Identification code	PahPh6 AP8358-100	
Chemical formula	$C_{22}H_{29}N_2SiY$	
Formula weight	438.47	
Temperature	100(2) K	
Wavelength	0.71073 Å	
Crystal size	0.126 x 0.178 x 0.234 mm	
Crystal habit	clear colourless fragment	
Crystal system	monoclinic	
Space group	P 1 21/n 1	
Unit cell dimensions	a = 10.4940(5) Å	$\alpha = 90°$
	b = 12.6978(6) Å	$\beta = 91.044(2)°$
	c = 15.9846(7) Å	$\gamma = 90°$
Volume	2129.61(17) $Å^3$	
Z	4	
Density (calculated)	1.368 g/cm^3	
Absorption coefficient	2.802 mm^{-1}	
F(000)	912	

Table S4. Data collection and structure refinement for compound **3**.

Diffractometer	Bruker D8 Venture Duo IMS	
Radiation source	IMS microsource, Mo	
Theta range for data collection	2.30 to 29.57°	
Index ranges	-14<=h<=14, -17<=k<=17, -22<=l<=22	
Reflections collected	66552	
Independent reflections	5978 [R(int) = 0.0934]	
Coverage of independent reflections	100.0%	
Absorption correction	Multi-Scan	
Max. and min. transmission	0.7190 and 0.5600	
Refinement method	Full-matrix least-squares on F^2	
Refinement program	SHELXL-2014/7 (Sheldrick, 2014)	
Function minimized	$\Sigma w(F_o^2 - F_c^2)^2$	
Data / restraints / parameters	5978 / 0 / 249	
Goodness-of-fit on F^2	1.041	
Δ/σ_{max}	0.002	
Final R indices	4877 data; $I>2\sigma(I)$	R1 = 0.0348, wR2 = 0.0645
	all data	R1 = 0.0534, wR2 = 0.0692
Weighting scheme	$w=1/[\sigma^2(F_o^2)+(0.0242P)^2+1.9235P]$ where $P=(F_o^2+2F_c^2)/3$	

Largest diff. peak and hole	0.461 and -0.386 eÅ^{-3}
R.M.S. deviation from mean	0.084 eÅ^{-3}

SC-XRD determination of compound 5 (CCDC 1936318)

A clear yellow fragment-like specimen of $C_{44}H_{70}Al_2N_4Si_2$, approximate dimensions 0.136 mm x 0.137 mm x 0.203 mm, was used for the X-ray crystallographic analysis. The X-ray intensity data were measured on a Bruker D8 Venture system equipped with a Helios optic monochromator and a Mo TXS rotating anode (λ = 0.71073 Å).

A total of 1443 frames were collected. The total exposure time was 3.56 hours. The frames were integrated with the Bruker SAINT software package using a narrow-frame algorithm. The integration of the data using a triclinic unit cell yielded a total of 42515 reflections to a maximum θ angle of 25.03° (0.84 Å resolution), of which 8029 were independent (average redundancy 5.295, completeness = 99.8%, R_{int} = 3.46%, R_{sig} = 2.41%) and 6684 (83.25%) were greater than $2\sigma(F^2)$. The final cell constants of $\underline{a}$ = 11.8436(4) Å, $\underline{b}$ = 12.0036(5) Å, $\underline{c}$ = 16.2833(6) Å, α = 87.653(2)°, β = 80.177(2)°, γ = 88.234(2)°, volume = 2278.41(15) Å^3, are based upon the refinement of the XYZ-centroids of 9290 reflections above 20 σ(I) with 4.930° < 2θ < 51.39°. Data were corrected for absorption effects using the Multi-Scan method (SADABS). The ratio of minimum to maximum apparent transmission was 0.915. The calculated minimum and maximum transmission coefficients (based on crystal size) are 0.9700 and 0.9800.

The final anisotropic full-matrix least-squares refinement on F^2 with 698 variables converged at R1 = 4.64%, for the observed data and wR2 = 11.77% for all data. The goodness-of-fit was 1.040. The largest peak in the final difference electron density synthesis was 0.346 e$^-$/Å^3 and the largest hole was -0.339 e$^-$/Å^3 with an RMS deviation of 0.048 e$^-$/Å^3. On the basis of the final model, the calculated density was 1.115 g/cm^3 and F(000), 832 e$^-$.

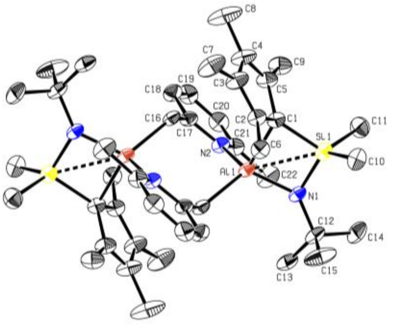

Figure S4. Ortep drawing with 50% ellipsoids for compound **5**.

Table S5. Sample and crystal data for compound **5**.

Identification code	WegMi6 AP9203-100	
Chemical formula	$C_{44}H_{70}Al_2N_4Si_2$	
Formula weight	255.06	
Temperature	100(2) K	
Wavelength	0.71073 Å	
Crystal size	0.136 x 0.137 x 0.203 mm	
Crystal habit	clear yellow fragment	
Crystal system	triclinic	
Space group	P -1	
Unit cell dimensions	a = 11.8436(4) Å	α = 87.653(2)°
	b = 12.0036(5) Å	β = 80.177(2)°
	c = 16.2833(6) Å	γ = 88.234(2)°
Volume	2278.41(15) Å^3	
Z	6	
Density (calculated)	1.115 g/cm^3	
Absorption coefficient	0.150 mm^{-1}	
F(000)	832	

Table S6. Data collection and structure refinement for compound **5**.

Diffractometer	Bruker D8 Venture	
Radiation source	TXS rotating anode, Mo	
Theta range for data collection	2.41 to 25.03°	
Index ranges	-14<=h<=14, -14<=k<=14, -19<=l<=19	
Reflections collected	42515	
Independent reflections	8029 [R(int) = 0.0346]	
Coverage of independent reflections	99.8%	
Absorption correction	Multi-Scan	
Max. and min. transmission	0.9800 and 0.9700	
Refinement method	Full-matrix least-squares on F^2	
Refinement program	SHELXL-2014/7 (Sheldrick, 2014)	
Function minimized	$\Sigma\ w(F_o^2 - F_c^2)^2$	
Data / restraints / parameters	8029 / 262 / 698	
Goodness-of-fit on F^2	1.040	
Δ/σ_{max}	0.001	
Final R indices	6684 data; $I>2\sigma(I)$	R1 = 0.0464, wR2 = 0.1086
	all data	R1 = 0.0592, wR2 = 0.1177
Weighting scheme	$w=1/[\sigma^2(F_o^2)+(0.0399P)^2+2.6556P]$ where $P=(F_o^2+2F_c^2)/3$	

Largest diff. peak and hole	0.346 and -0.339 eÅ^{-3}
R.M.S. deviation from mean	0.048 eÅ^{-3}

SC-XRD determination of compound 7 (CCDC 1936315)

A clear colourless fragment-like specimen of $C_{22}H_{29}AlN_2Si$, approximate dimensions 0.126 mm x 0.183 mm x 0.389 mm, was used for the X-ray crystallographic analysis. The X-ray intensity data were measured on a Bruker D8 Kappa Apex II system equipped with a Triumph monochromator monochromator and a Mo fine-focus sealed tube (λ = 0.71073 Å).

A total of 2682 frames were collected. The total exposure time was 3.73 hours. The frames were integrated with the Bruker SAINT software package using a narrow-frame algorithm. The integration of the data using a triclinic unit cell yielded a total of 35367 reflections to a maximum θ angle of 25.03° (0.84 Å resolution), of which 4254 were independent (average redundancy 8.314, completeness = 99.8%, R_{int} = 3.56%, R_{sig} = 2.35%) and 3524 (82.84%) were greater than $2\sigma(F^2)$. The final cell constants of $\underline{a}$ = 9.558(2) Å, $\underline{b}$ = 9.687(2) Å, $\underline{c}$ = 13.866(3) Å, α = 106.254(9)°, β = 94.156(9)°, γ = 100.572(9)°, volume = 1201.1(5) Å^3, are based upon the refinement of the XYZ-centroids of 116 reflections above 20 σ(I) with 4.362° < 2θ < 47.95°. Data were corrected for absorption effects using the Multi-Scan method (SADABS). The ratio of minimum to maximum apparent transmission was 0.950. The calculated minimum and maximum transmission coefficients (based on crystal size) are 0.9470 and 0.9820.

The final anisotropic full-matrix least-squares refinement on F^2 with 241 variables converged at R1 = 3.46%, for the observed data and wR2 = 8.68% for all data. The goodness-of-fit was 1.036. The largest peak in the final difference electron density synthesis was 0.272 e$^-$/Å^3 and the largest hole was -0.232 e$^-$/Å^3 with an RMS deviation of 0.040 e$^-$/Å^3. On the basis of the final model, the calculated density was 1.041 g/cm^3 and F(000), 404 e$^-$.

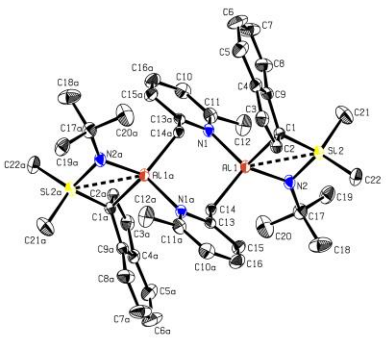

Figure S5. Ortep drawing with 50% ellipsoids for compound **7**.

Table S7. Sample and crystal data for compound **7**.

Identification code	SchFa2 AP7596-100	
Chemical formula	$C_{22}H_{29}AlN_2Si$	
Formula weight	376.54	
Temperature	100(2) K	
Wavelength	0.71073 Å	
Crystal size	0.126 x 0.183 x 0.389 mm	
Crystal habit	clear colourless fragment	
Crystal system	triclinic	
Space group	P -1	
Unit cell dimensions	a = 9.558(2) Å	α = 106.254(9)°
	b = 9.687(2) Å	β = 94.156(9)°
	c = 13.866(3) Å	γ = 100.572(9)°
Volume	1201.1(5) $Å^3$	
Z	2	
Density (calculated)	1.041 g/cm^3	
Absorption coefficient	0.141 mm^{-1}	
F(000)	404	

Table S8. Data collection and structure refinement for compound **7**.

Diffractometer	Bruker D8 Kappa Apex II	
Radiation source	fine-focus sealed tube, Mo	
Theta range for data collection	2.19 to 25.03°	
Index ranges	-11<=h<=11, -11<=k<=11, -16<=l<=16	
Reflections collected	35367	
Independent reflections	4254 [R(int) = 0.0356]	
Coverage of independent reflections	99.8%	
Absorption correction	Multi-Scan	
Max. and min. transmission	0.9820 and 0.9470	
Refinement method	Full-matrix least-squares on F^2	
Refinement program	SHELXL-2014/7 (Sheldrick, 2014)	
Function minimized	$\Sigma\ w(F_o^2 - F_c^2)^2$	
Data / restraints / parameters	4254 / 0 / 241	
Goodness-of-fit on F^2	1.036	
Final R indices	3524 data; $I>2\sigma(I)$	R1 = 0.0346, wR2 = 0.0811
	all data	R1 = 0.0447, wR2 = 0.0868
Weighting scheme	$w=1/[\sigma^2(F_o^2)+(0.0349P)^2+0.6634P]$ where $P=(F_o^2+2F_c^2)/3$	
Largest diff. peak and hole	0.272 and -0.232 $eÅ^{-3}$	

R.M.S. deviation from mean 0.040 eÅ^{-3}

3. Polymerization Studies and Mechanism Elucidation

Further polymerization experiments in addition to Table 1:

Table S9. Catalytic conversion of DEVP with the synthesized CGCs.(a)

Run	Catalyst	V_{tol} / mL	t / min	Yield / % (b)	M_n / 10^3 g/mol (c)	Đ (M_w/M_n)	I / % (d)	TOF / h^{-1}
1	**1-CH_2TMS**	20	1	100	150	1.19	32	18,000
2	**2-CH_2TMS**	20	1	100	450	1.26	11	18,000
3	**5**	3	45	91	160	1.83	28	360
4	**6**	3	45	38	160	1.67	10	150
5	**7**	3	45	98	100	2.28	48	400

(a) V_{DEVP} = 1.0 mL, T = 30 °C, [M]/[CGC] = 300/1, (b) measured gravimetrically and by NMR spectroscopy (^{31}P NMR spectroscopy), (c) determined by GPC-MALS in H_2O / THF (9 g/L tetrabutylammonium bromide), (d) initiator efficiency ($M_{n(theo.)}/M_{n(determ.)}$).

End group analysis via ESI-MS:

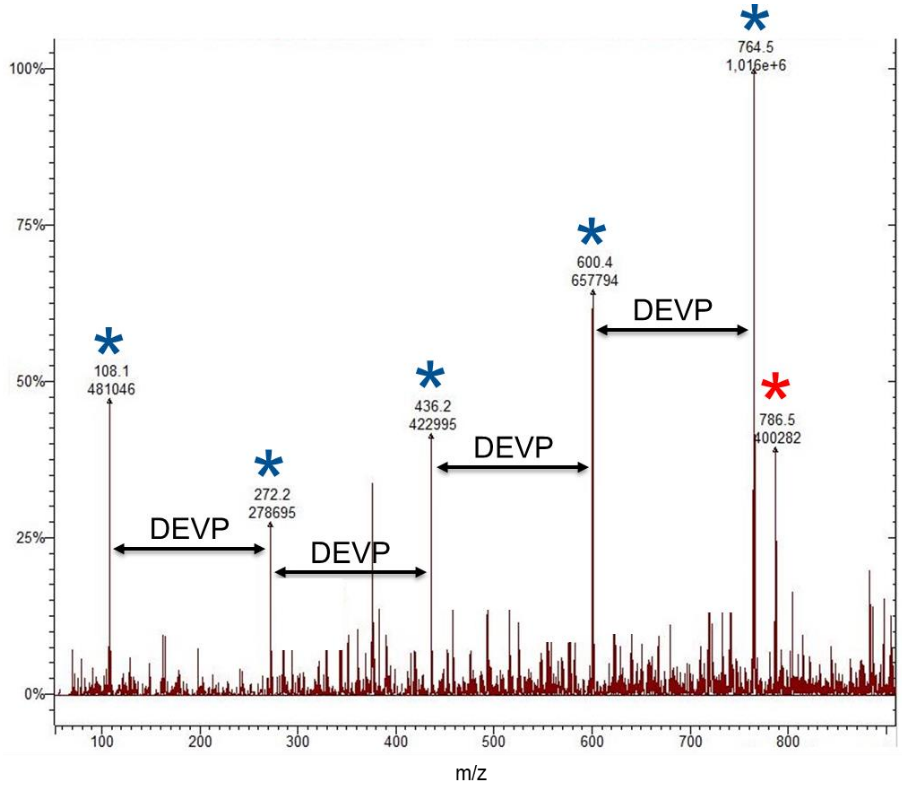

Figure S6. ESI MS spectrum of DEVP oligomers produced with **5**. One major series of peaks is evident: m/z = n × M_{Mon} +M_H + M_{Lut} (blue); M_{Mon} = 164, end groups: M_{Lut} = 107. Red peak: m/z = n × M_{Mon} +M_{Na} + M_{Lut}; M_{Mon} = 164, end groups: M_{Lut} = 107.

Living polymerization behaviour (CGC 5):

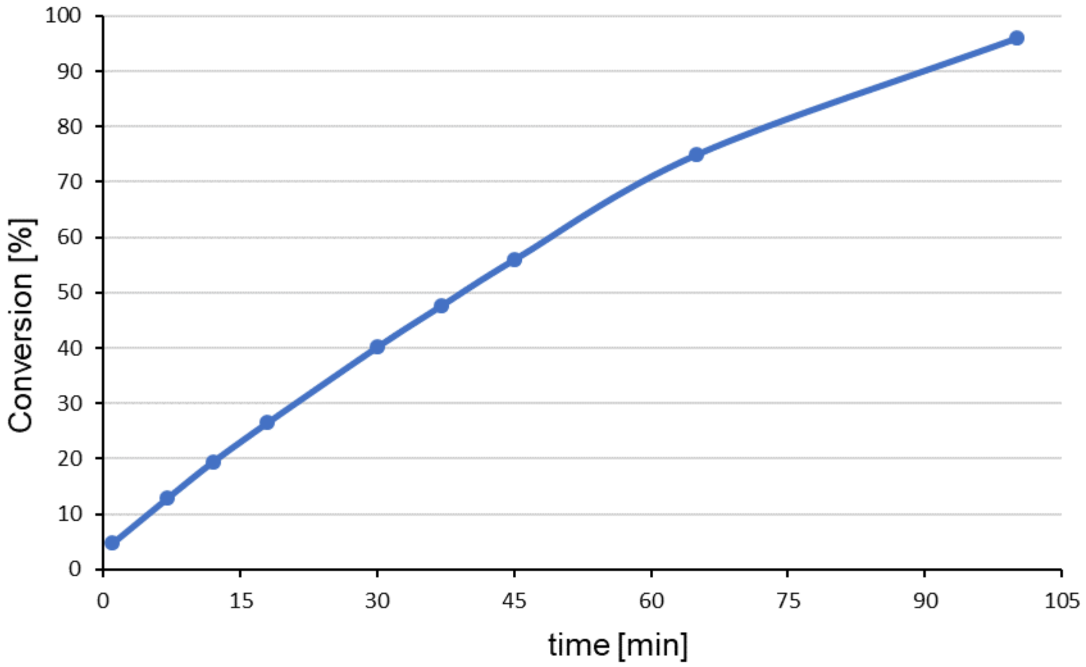

Figure S7. Time vs. conversion plot for polymerization of diethylvinylphosphonate with **5** (Monomer to catalyst ratio of 300/1, r.t., 5 mL toluene, 0.5 mL DEVP).

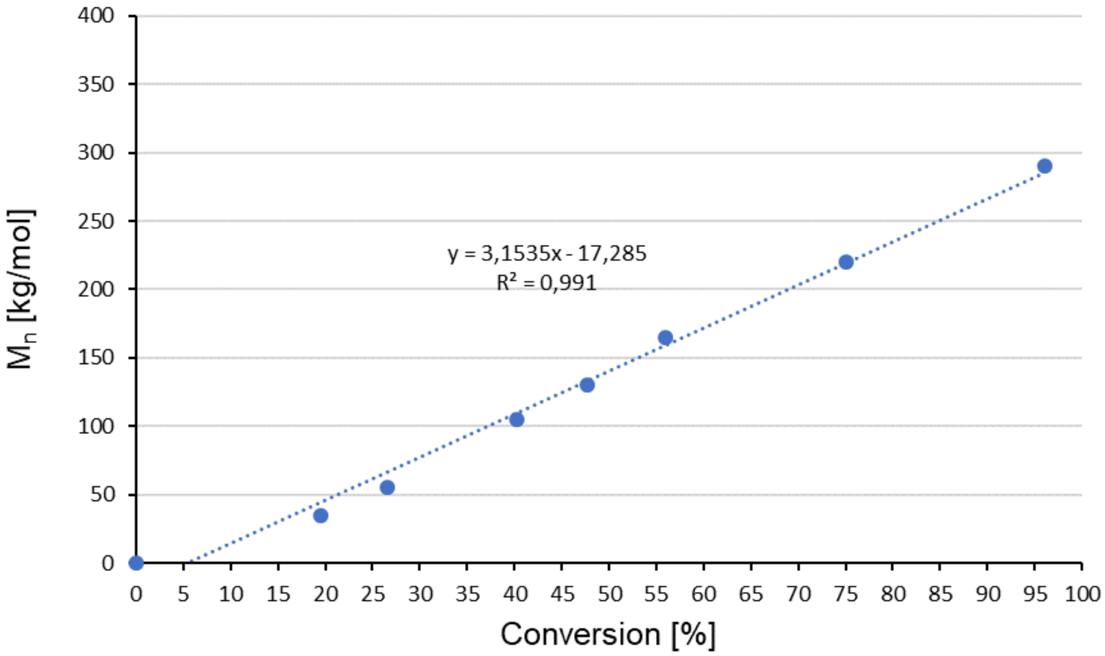

Figure S8. Linear growth of the molecular weight with increasing conversion.

Determination of catalyst order (differential method):

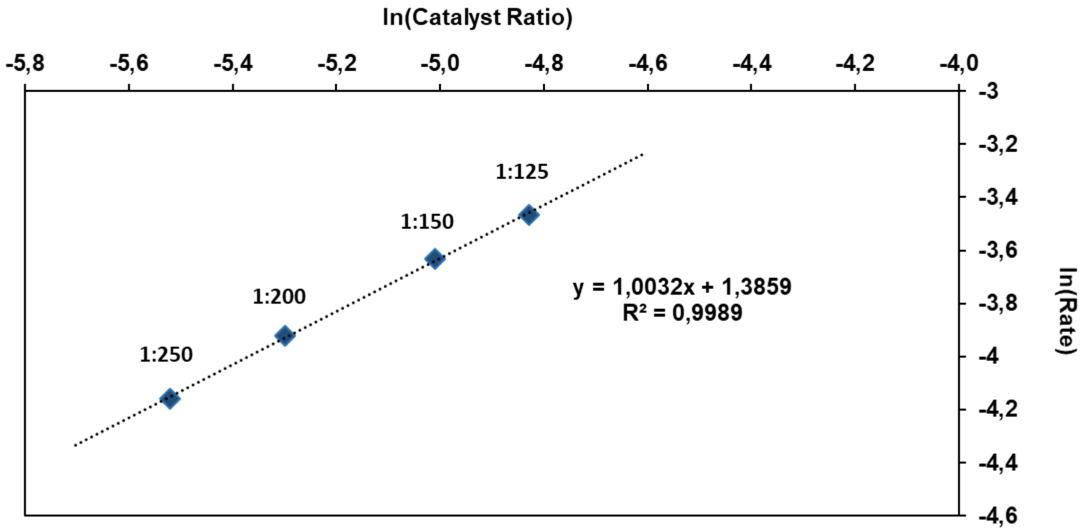

Figure S9. Determination of catalyst order: catalyst **5**, 0.15 mL DEVP, 0.75 mL C_6D_6, 25 °C.

Determination of monomer order (tangential method):

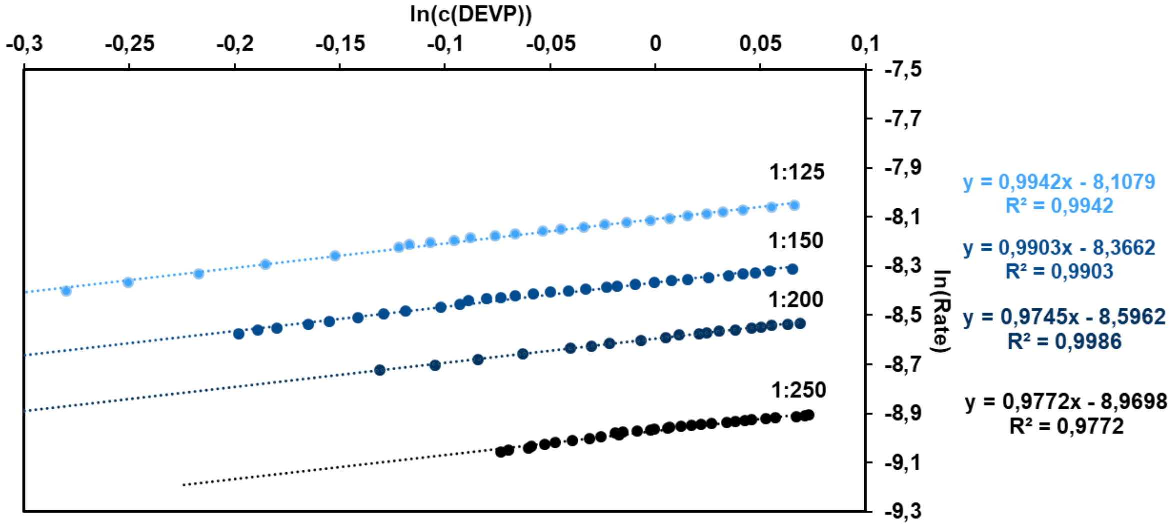

Figure S10. Determination of monomer order: catalyst **5**, 0.15 mL DEVP, 0.75 mL C_6D_6, 25 °C.

Living polymerization behaviour (CGC 1):

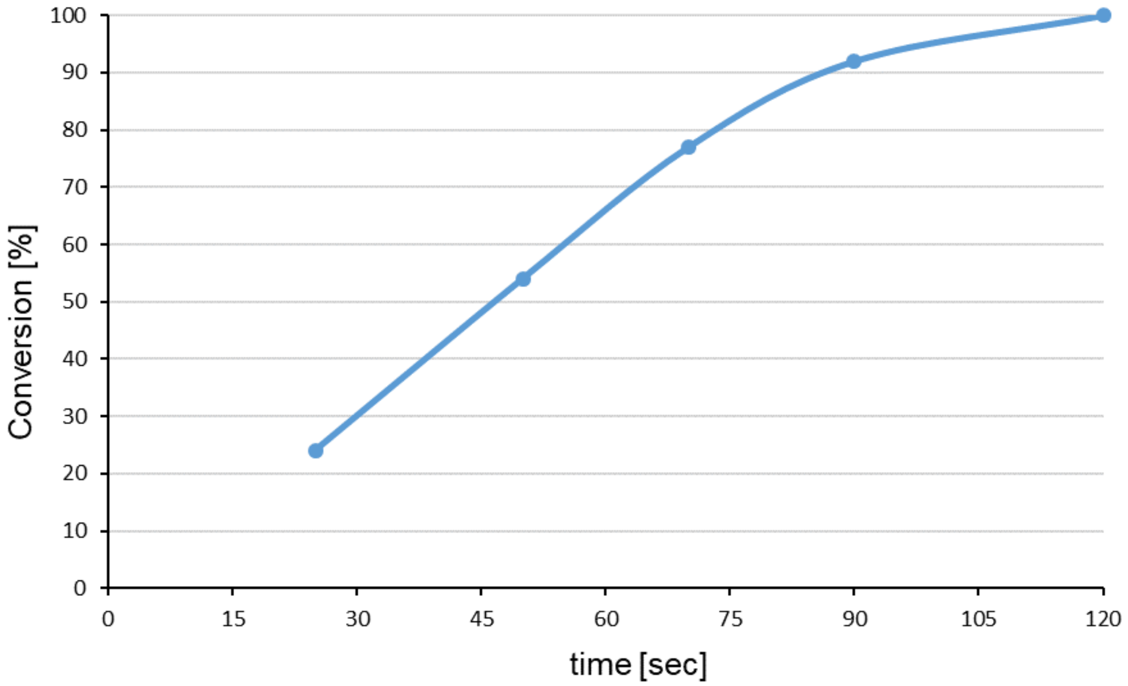

Figure S11. Time vs. conversion plot for polymerization of diethylvinylphosphonate with **1** (Monomer to catalyst ratio of 300/1, −30 °C, 20 mL toluene, 1 mL DEVP).

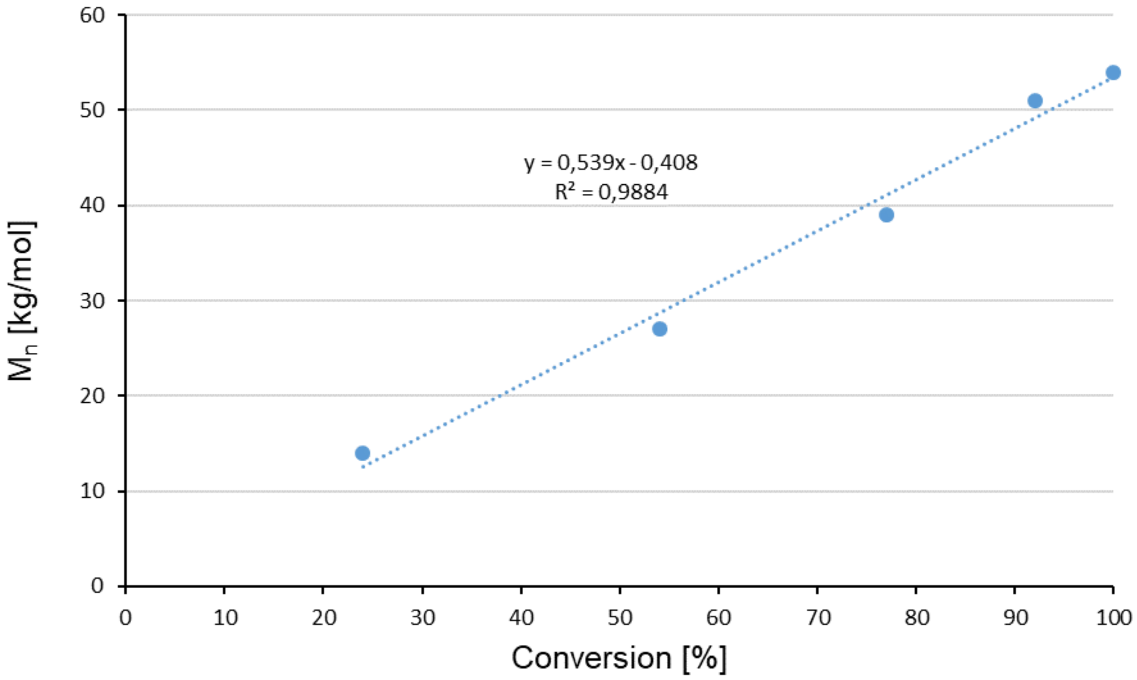

Figure S12. Linear growth of the molecular weight with increasing conversion.

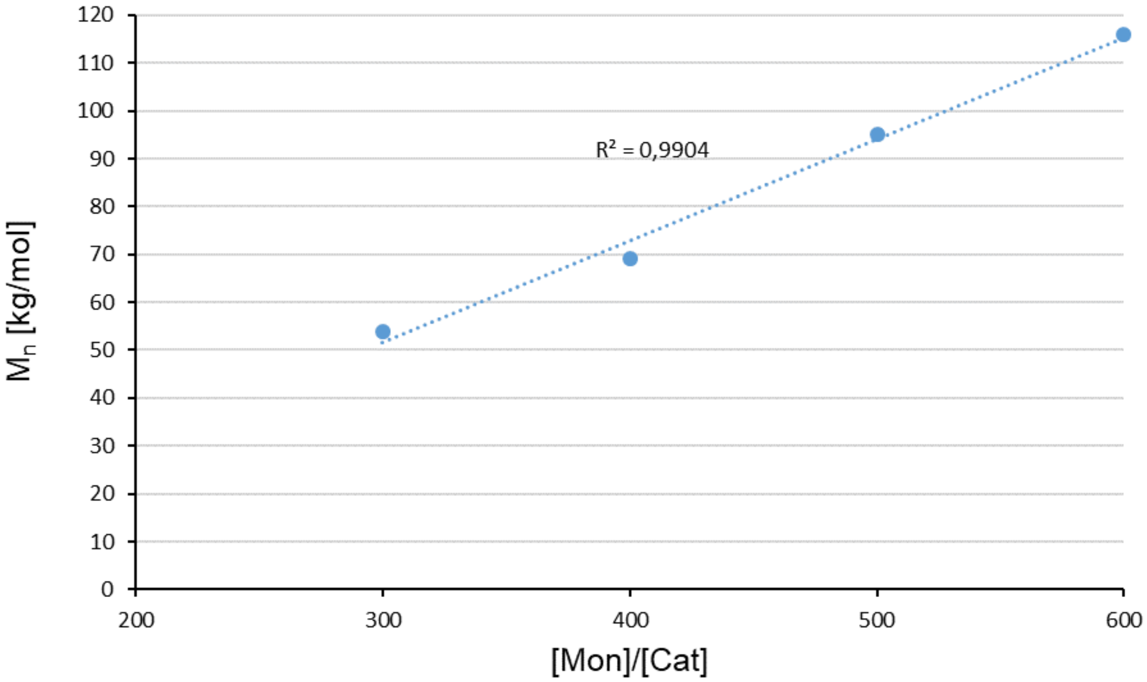

Figure S13. Molecular weight vs. [Mon]/[Cat] plot for polymerization of diethylvinylphosphonate with **1** ensuring quantitative conversions (−30 °C, 20 mL toluene, 1 mL DEVP).

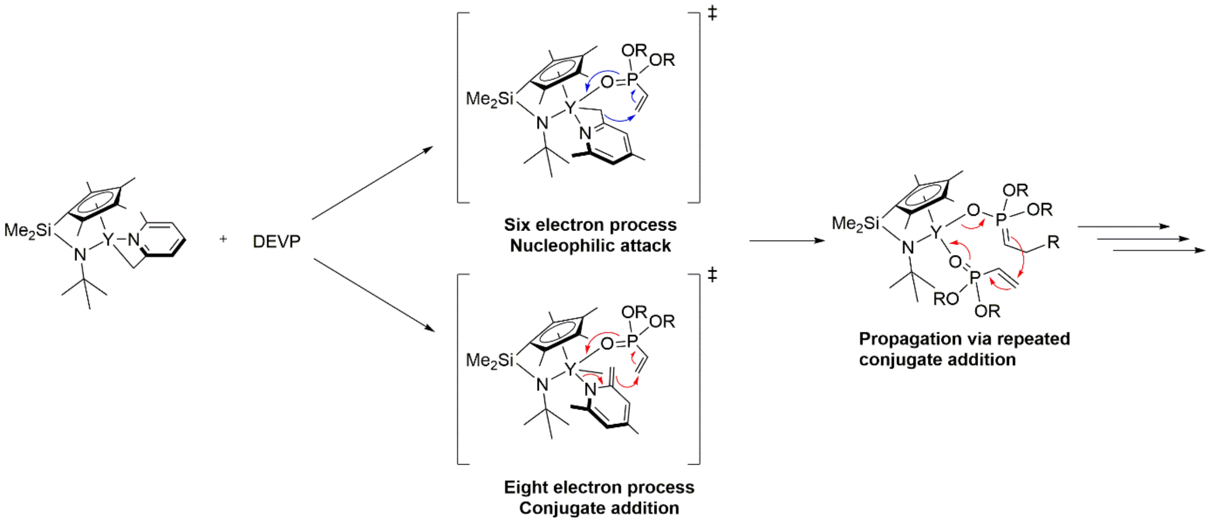

Scheme S1. Proposed initiation reaction via nucleophilic transfer (six electron process, blue) or conjugate addition (eight electron process, red) and propagation via a repeated conjugate addition of the polymer chain to the coordinated monomer at the metal center by the example of catalyst **1**.

4. NMR, GPC and Thermal Analysis of the PDEVP Samples

Comparison of the $^{31}P\{^1H\}$ NMR spectra:

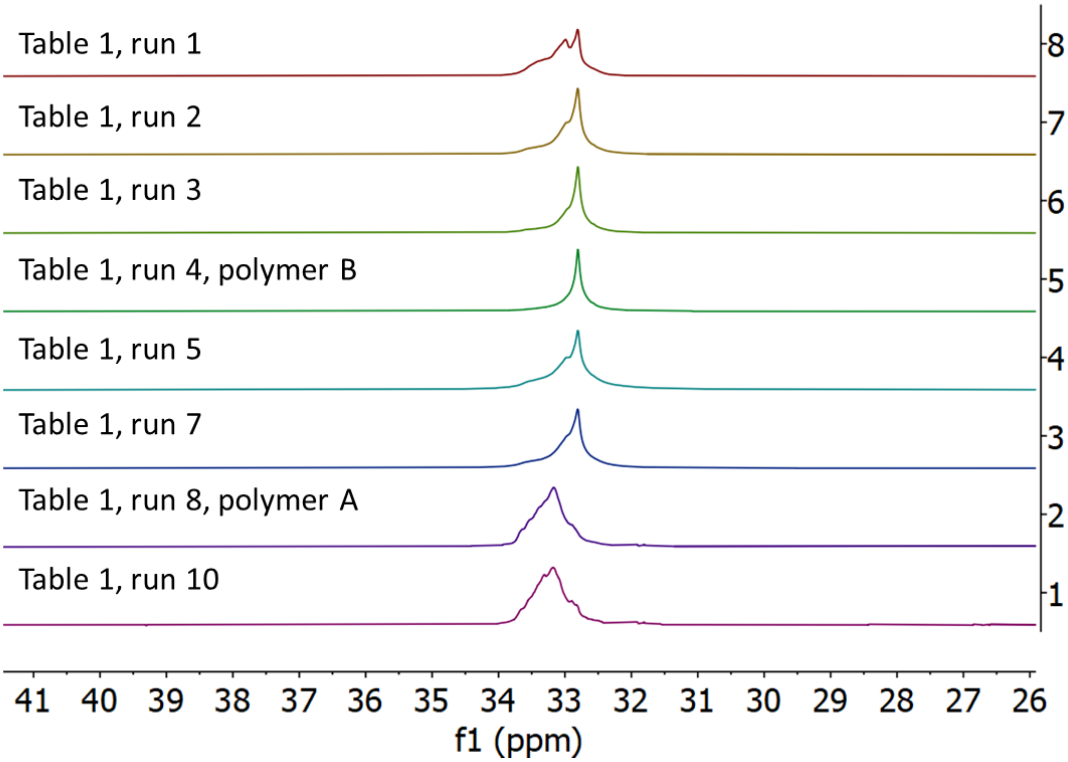

Figure S14. $^{31}P\{^1H\}$ NMR spectra of the discussed polymers in MeOD$_4$.

NMR spectra, thermal characteristics & GPC trace of Table 1, run 4 (polymer B):

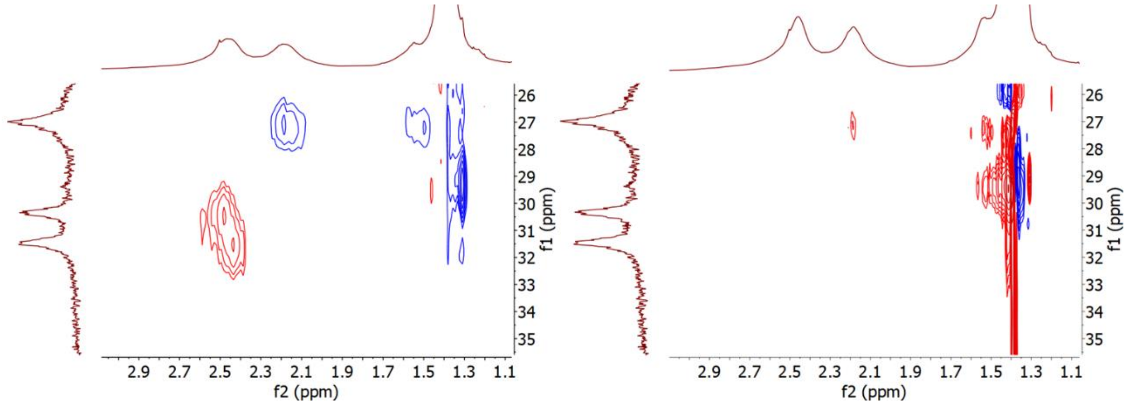

Figure S15. Phase-sensitive ^1H-^{13}C DEPT-edited HSQC vs. a ^1H-^{13}C-^{31}P triple resonance HCP 2D experiment edited by J_{PC} = 20 Hz (for details see Table S10).

Table S10. Pulseprogram parameters for ^{1}H-^{13}C-^{31}P triple resonance HCP 2D experiment edited by J_{PC} = 20 Hz (Figure S12).

General

PULPROG	na_hcpqetgpsi.1	
TD	2048	
SWH [Hz, ppm]	2380.95	5.94894
AQ [sec]	0.4300800	
RG	101	
DW [µsec]	210.000	
DE [µsec]	6.50	
CNST2 (J(HC))	140.0000000	
CNST5 (J(CP))	20.0000000	
CNST11	8.0000000	For multiplicity selection = 4 for CH, 8 for all
d0 [sec]	0.00000300	
D1 [sec]	2.000000000	
d4 [sec]	0.00178571	
d11 [sec]	0.03000000	
d12 [sec]	0.00002000	
d13 [sec]	0.00000400	
D16 [sec]	0.000200000	
d20 [sec]	0.00500000	
d22 [sec]	0.00625000	
d24 [sec]	0.00089286	
DELTA1 [sec]	0.00505000	
DELTA2 [sec]	0.00499700	
DELTA3 [sec]	0.00120800	
DELTA4 [sec]	0.00500000	
DS	128	
in0 [sec]	0.00008280	
in20 [sec]	0.00008280	
INF1 [µsec]	165.60	
NS	256	
TAU [sec]	0.00002500	
TDav	0	
Channel f1		
SFO1 [MHz]	400.2312007	
O1 [Hz, ppm]	1200.69	3.000
NUC1	1H	
P1 [µsec]	10.000	
p2 [µsec]	20.00	
P28 [µsec]	1000.000	
PLW1 [W, dB]	9.604	-9.82
O2 [Hz, ppm]	4025.52	40.000

NUC2	13C	
CPDPRG 2	garp4	
P3 [µsec]	20.000	
p4 [µsec]	40.00	
PCPD2 [µsec]	80.00	
PLW2 [W, dB]	52.44	-17.20
PLW12 [W, dB]	3.2775	-5.16
Channel f3		
SFO3 [MHz]	162.0210965	
O3 [Hz, ppm]	5022.50	31.000
NUC3	31P	
CPDPRG 3	garp4	
P21 [µsec]	25.000	
p22 [µsec]	50.00	
PCPD3 [µsec]	100.00	
PLW3 [W, dB]	15.924	-12.02
PLW16 [W, dB]	0.99525	0.02
Gradient channel		
GPNAM 1	SMSQ10.100	
GPZ1 [%]	40.00	
GPNAM 2	SMSQ10.100	
GPZ2 [%]	25.00	
GPNAM 3	SMSQ10.100	
GPZ3 [%]	40.00	
GPNAM 4	SMSQ10.100	
GPZ4 [%]	20.10	
P16 [µsec]	1000.000	

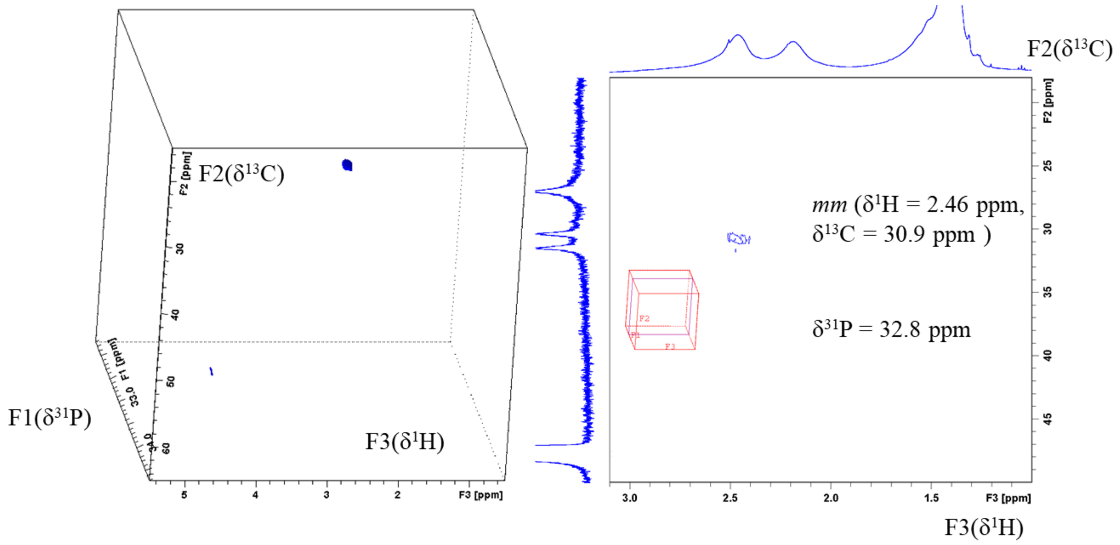

Figure S16. ^{1}H-^{13}C-^{31}P triple resonance HCP 3D experiment edited by J_{PC} = 110 Hz (for details see Table S11, S12).

Table S11. Pulseprogram for ^{1}H-^{13}C-^{31}P triple resonance HCP 3D experiment edited by J_{PC} = 110 Hz (Figure S13, SX).

```
;hcp3d_gg              03.03.2019/gg
;ex hcacogp3d
;avance-version (12/01/11)
;3D sequence with
;   inverse correlation for triple resonance using multiple
;      inept transfer steps
;
;      F1(H) -> F2(C) -> F2'(P, t1) -> F2(C, t2) -> F1(H,t3)
;
;on/off resonance Ca and C=O pulses using shaped pulse
;phase sensitive (t1)
;phase sensitive using Echo/Antiecho-TPPI gradient selection (t2)
;
;(L.E. Kay et al., J. Magn. Reson 89, 496 - 514 (1990))
;
;$CLASS=HighRes
;$DIM=3D
;$TYPE=
;$SUBTYPE=
;$COMMENT=


prosol relations=<triple>


#include <Avance.incl>
#include <Grad.incl>
#include <Delay.incl>


"p2=p1*2"
"p4=p3*2"
"p22=p21*2"
```

```
"d11=30m"
"d12=20u"
"d13=4u"

"d22=0.25/cnst21"

"d0=3u"
"d10=3u"

"in0=inf1/2"
"in10=inf2/2"


"DELTA=d0*2+larger(p4,p2)"
"DELTA1=d22-d21-p2-p4/2-p16-4u"
"DELTA2=d22-p4/2-p16-4u"
"DELTA3=d22-p4/2"
"DELTA4=d22-d21-p2-p4/2-d10*2"
"DELTA5=d21-p16-d16"
"DELTA6=d4-p16-d16-8u"



aqseq 321


1 d11 ze
  d11 pl1:f1

  d11 pl3:f3
2 d11 do:f2
3 d1
  p1 ph1
  d4 pl2:f2
  (center (p2 ph1) (p4 ph2):f2)
  d4
  (p1 ph2) (p3 ph3):f2

  d21 UNBLKGRAD
  p2 ph1
  4u
  p16:gp1
  DELTA1
  (center (p4 ph1):f2 (p22 ph1):f3)
  4u
  p16:gp2
  DELTA2
  (p3 ph1):f2

  d13

  (p21 ph4):f3
  d0
  (center (p2 ph1) (p4 ph1):f2)
  d0
  (p22 ph1):f3
  DELTA
  (p21 ph1):f3

  d13
```

```
   (p3 ph5):f2
   DELTA3
   (p4 ph1):f2
   d10
   (p22 ph1):f3
   DELTA4
   p2 ph1
   p16:gp3*EA
   d16
   DELTA5
   d10

   (ralign (p1 ph1) (p3 ph6):f2 )
   d4
   (center (p2 ph1) (p4 ph1):f2 )
   4u
   p16:gp4
   d16
   DELTA6 pl12:f2
   4u BLKGRAD
   go=2 ph31 cpd2:f2
   d11 do:f2 mc #0 to 2
      F1PH(calph(ph4, +90), caldel(d0, +in0))
      F2EA(calgrad(EA), caldel(d10, +in10) & calph(ph5, +180) &
calph(ph31, +180))
exit


ph1 = 0
ph2 = 1
ph3 = 0 2
ph4 = 0 0 2 2
ph5 = 0 0 0 0 2 2 2 2
ph6 = 0 0 0 0 0 0 0 0 2 2 2 2 2 2 2 2
ph31= 0 2 2 0 2 0 0 2 2 0 0 2 0 2 2 0


;pl1 : f1 channel - power level for pulse (default)
;pl2 : f2 channel - power level for pulse (default)
;pl3 : f3 channel - power level for pulse (default)
;pl12: f2 channel - power level for CPD/BB decoupling
;p1 : f1 channel -  90 degree high power pulse
;p2 : f1 channel - 180 degree high power pulse
;p3: f2 channel -  90 degree shaped pulse
;p4: f2 channel - 180 degree shaped pulse
;p16: homospoil/gradient pulse                         [1 msec]
;p21: f3 channel -  90 degree high power pulse
;p22: f3 channel - 180 degree high power pulse
;d0 : incremented delay (F1 in 3D)                     [3 usec]
;d1 : relaxation delay; 1-5 * T1
;d4 : 1/(4J(HC))                                      [1.7 msec]
;d10: incremented delay (F2 in 3D)                     [3 usec]
;d11: delay for disk I/O                               [30 msec]
;d12: delay for power switching                        [20 usec]
;d13: short delay                                      [4 usec]
;d16: delay for homospoil/gradient recovery
;d21: 1/(4J`(HC)) or 1/(6J`(HC)) for CH or CH & CH2    [1.7 msec or 1.2
msec]
```

```
;d22: 1/(4J(13C,31P))
;cnst21: 1J(13C,31P)
;inf1: 1/SW(31P) = 2 * DW(31P)
;inf2: 1/SW(13C) = 2 * DW(13C)
;in0: 1/(2 * SW(31P) = DW(31P)
;nd0: 2
;in10: 1/(2 * SW(13C)) = DW(13C)
;nd10: 2
;ns: 16 * n
;ds: 32
;td1: number of experiments in F1
;td2: number of experiments in F2
;FnMODE: States-TPPI (or TPPI) in F1
;FnMODE: echo-antiecho in F2
;cpd2: decoupling according to sequence defined by cpdprg2
;pcpd2: f2 channel - 90 degree pulse for decoupling sequence


;use gradient ratio:    gp 1 : gp 2 : gp 3 : gp 4
;                          3 :    3 :   80 : 20.1

;for z-only gradients:
;gpz1: 3%
;gpz2: 3%
;gpz3: 80%
;gpz4: 20.1%

;use gradient files:
;gpnam1: SMSQ10.100
;gpnam2: SMSQ10.100
;gpnam3: SMSQ10.100
;gpnam4: SMSQ10.100



;$Id: hcacogp3d,v 1.9 2012/01/31 17:49:23 ber Exp $
```

Table S12. Pulseprogram parameters for ^{1}H-^{13}C-^{31}P triple resonance HCP 3D experiment edited by J_{PC} = 110 Hz (Figure S13, SX).

General		
PULPROG	hcp3d_gg	
TD	2048	
SWH [Hz, ppm]	2000.00	4.99711
AQ [sec]	0.5120000	
RG	101	
DW [μsec]	250.000	
DE [μsec]	6.50	
CNST21 (1J13C,31P)	110.0000000	
d0 [sec]	0.00000300	
D1 [sec]	2.000000000	
D4 [sec]	0.001700000	
d10 [sec]	0.00000300	

d11 [sec]	0.03000000	
d13 [sec]	0.00000400	
D16 [sec]	0.000200000	
D21 [sec]	0.001200000	
d22 [sec]	0.00227273	
DELTA [sec]	0.00004600	
DELTA1 [sec]	0.00002873	
DELTA2 [sec]	0.00124873	
DELTA3 [sec]	0.00225273	
DELTA4 [sec]	0.00102673	
DELTA5 [sec]	0	
DELTA6 [sec]	0.00049200	
DS	32	
in0 [sec]	0.00102870	
in10 [sec]	0.00009940	
INF1 [µsec]	2057.40	
INF2 [µsec]	198.80	
NS	48	
TDav	0	
Channel f1		
SFO1 [MHz]	400.2312007	
O1 [Hz, ppm]	1200.69	3.000
NUC1	1H	
P1 [µsec]	10.000	
p2 [µsec]	20.00	
PLW1 [W, dB]	9.604	-9.82
Channel f2		
SFO2 [MHz]	100.6419395	
O2 [Hz, ppm]	4025.52	40.000
NUC2	13C	
CPDPRG 2	garp4	
P3 [µsec]	20.000	
p4 [µsec]	40.00	
PCPD2 [µsec]	80.00	
PLW2 [W, dB]	52.44	-17.20
PLW12 [W, dB]	3.2775	-5.16
Channel f3		
SFO3 [MHz]	162.0214529	
O3 [Hz, ppm]	5378.93	33.200
NUC3	31P	
P21 [µsec]	25.000	
p22 [µsec]	50.00	
PLW3 [W, dB]	15.924	-12.02
Gradient channel		
GPNAM 1	SMSQ10.100	
GPZ1 [%]	3.00	

GPNAM 2	SMSQ10.100
GPZ2 [%]	3.00
GPNAM 3	SMSQ10.100
GPZ3 [%]	80.00
GPNAM 4	SMSQ10.100
GPZ4 [%]	20.10
P16 [µsec]	1000.000

Peak	Area
2.78 ppm (*rr*)	~0
2.57 ppm (*mr*)	~0
2.45 ppm (*mm*)	1.000
2.27 ppm (*rmr*)	~0
2.19/2.14 ppm	1.000
1.55 ppm (*mmm*)	1.000
1.49 ppm (*mmr*)	~0
1.25 ppm (*rmr*)	~0

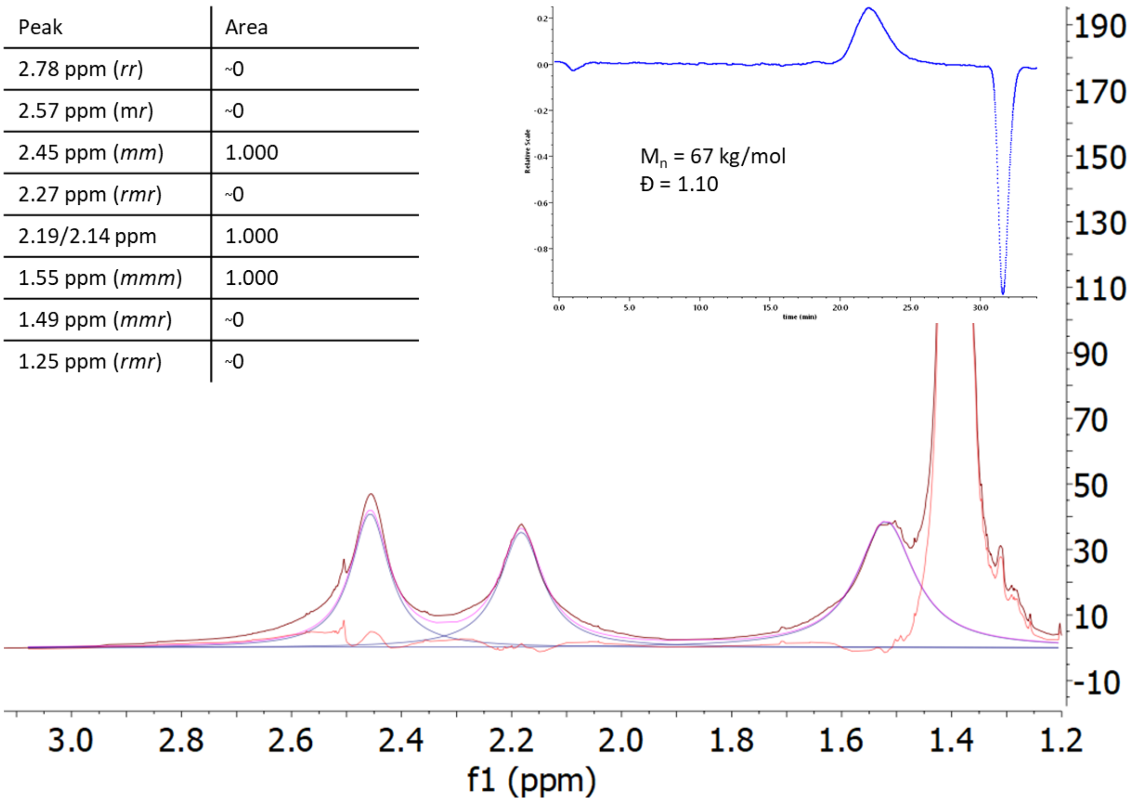

Figure S17. Quantification of the *mmm* tetrads with the line fitting method of MestReNova version 14.0.0-23239 and the GPC trace. Color coding: dark red – original spectrum, blue – peaks, pink – sum, red – residue.

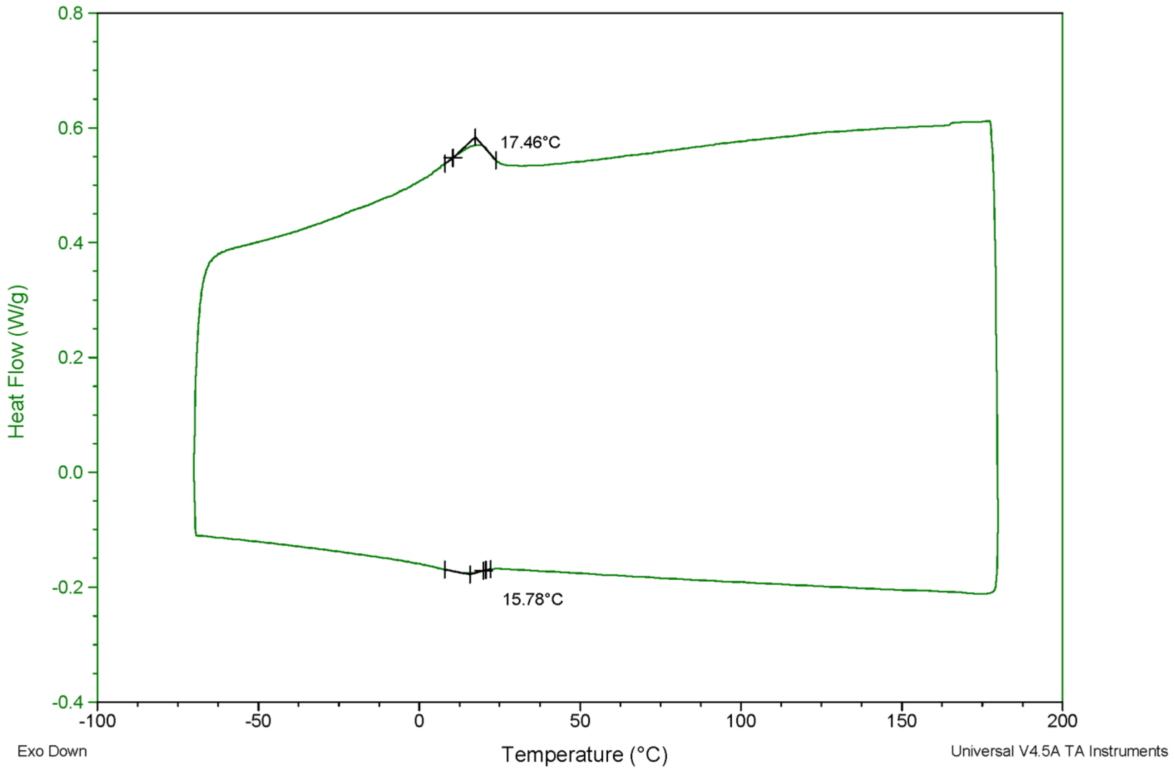

Figure S18. DSC analysis of polymer **B** showing a melting and crystallization point.

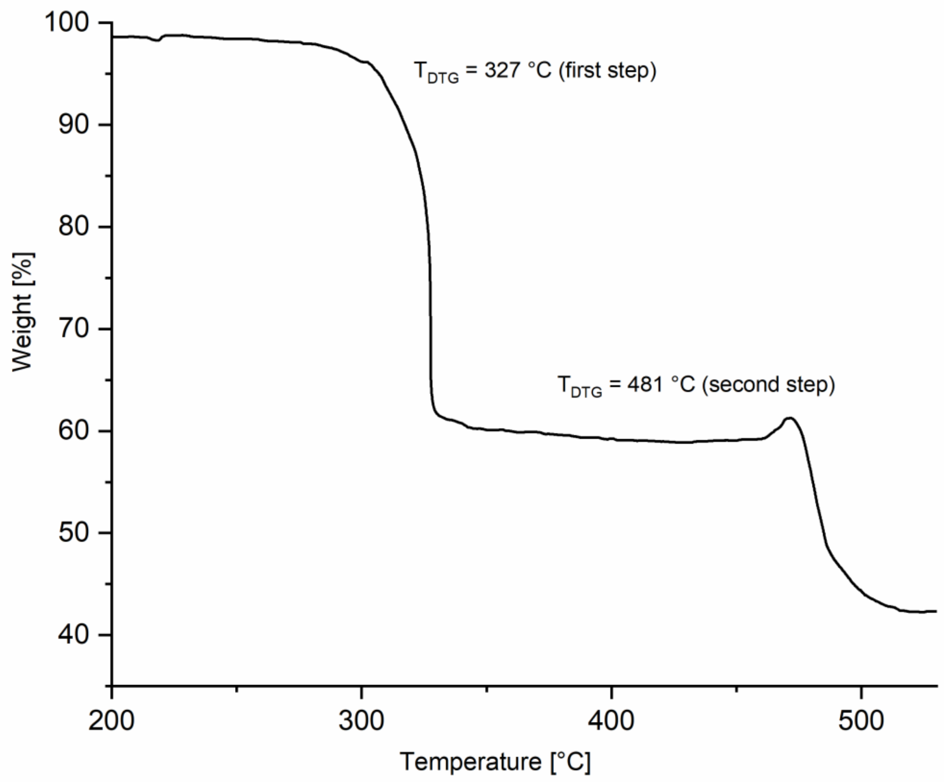

Figure S19. Thermogravimetric analysis of polymer **B**.

NMR spectra & GPC trace of Table 1, run 1:

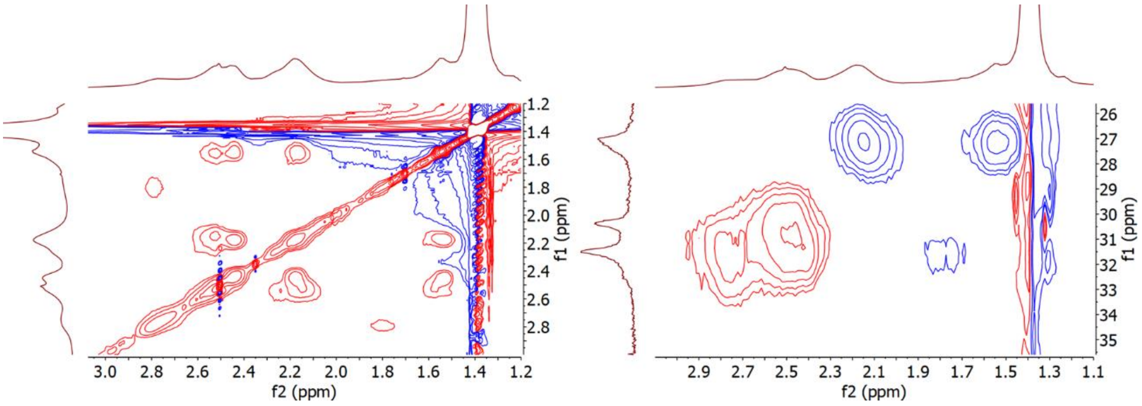

Figure S20. Phase-sensitive ^{1}H-^{13}C DEPT-edited HSQC (right) and TOCSY{^{31}P} NMR spectra in MeOD$_4$.

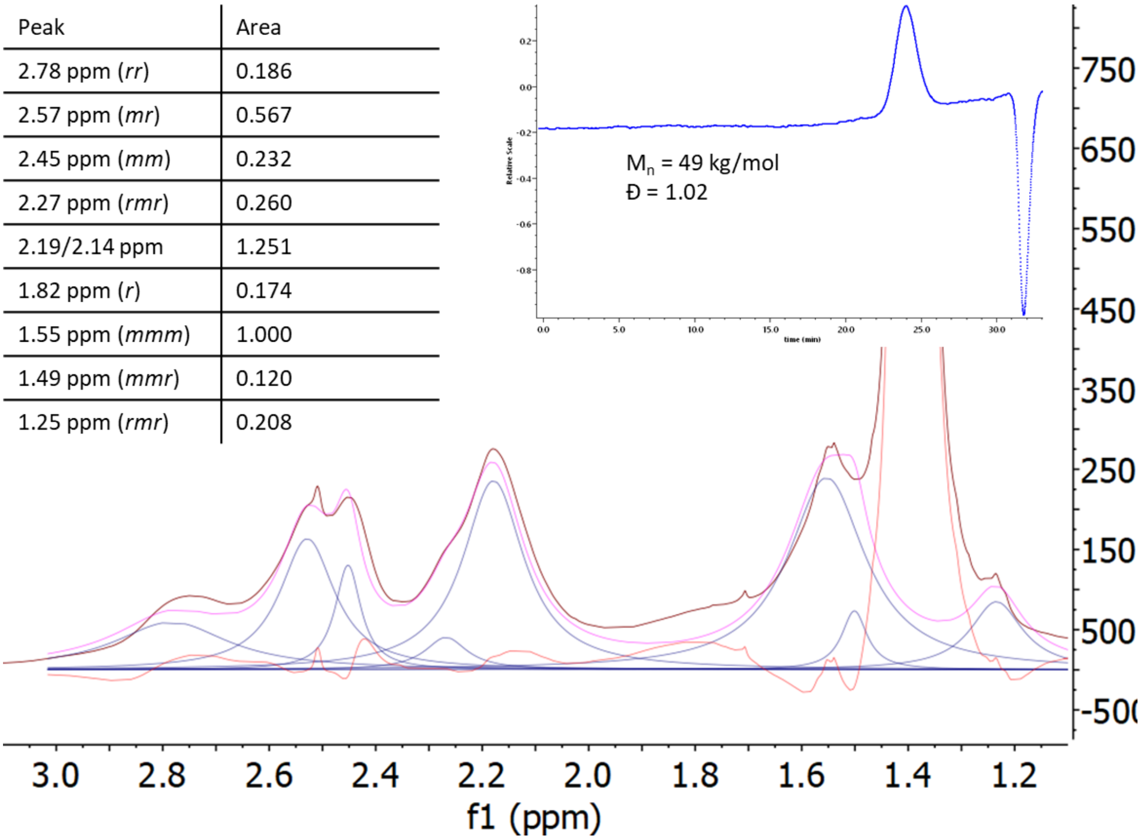

Peak	Area
2.78 ppm (*rr*)	0.186
2.57 ppm (*mr*)	0.567
2.45 ppm (*mm*)	0.232
2.27 ppm (*rmr*)	0.260
2.19/2.14 ppm	1.251
1.82 ppm (*r*)	0.174
1.55 ppm (*mmm*)	1.000
1.49 ppm (*mmr*)	0.120
1.25 ppm (*rmr*)	0.208

Figure S21. Quantification of the *mmm* tetrads with the line fitting method of MestReNova version 14.0.0-23239 and the GPC trace. Color coding: dark red – original spectrum, blue – peaks, pink – sum, red – residue.

NMR spectra & GPC trace of Table 1, run 2:

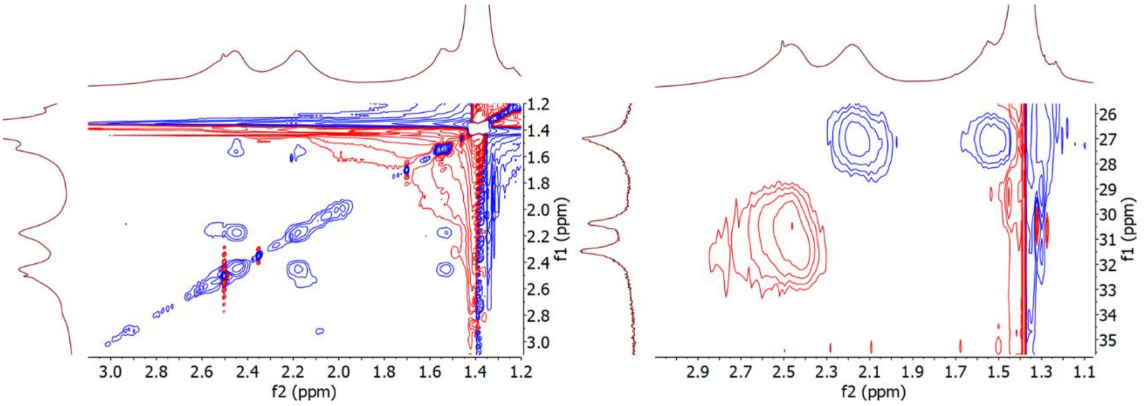

Figure S22. Phase-sensitive ^{1}H-^{13}C DEPT-edited HSQC (right) and TOCSY{^{31}P} NMR spectra in MeOD$_4$.

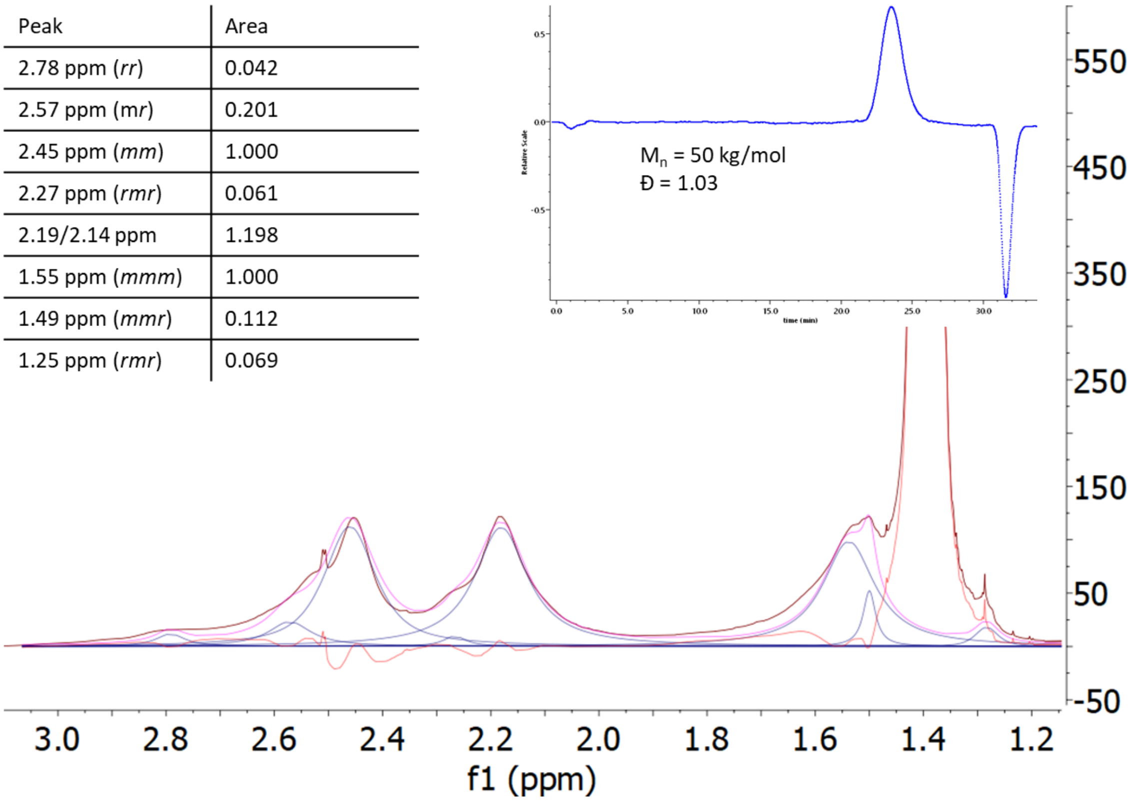

Peak	Area
2.78 ppm (*rr*)	0.042
2.57 ppm (mr)	0.201
2.45 ppm (*mm*)	1.000
2.27 ppm (*rmr*)	0.061
2.19/2.14 ppm	1.198
1.55 ppm (*mmm*)	1.000
1.49 ppm (*mmr*)	0.112
1.25 ppm (*rmr*)	0.069

Figure S23. Quantification of the *mmm* tetrads with the line fitting method of MestReNova version 14.0.0-23239 and the GPC trace. Color coding: dark red – original spectrum, blue – peaks, pink – sum, red – residue.

NMR spectra & GPC trace of Table 1, run 3:

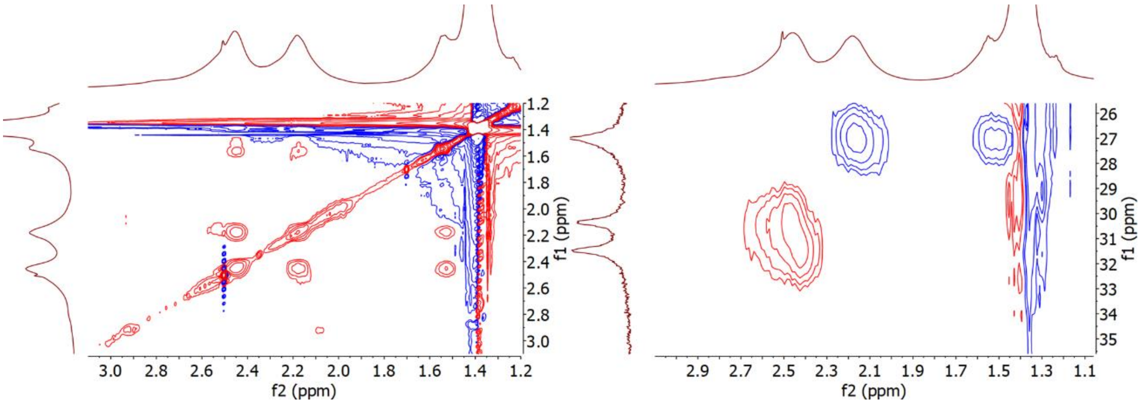

Figure S24. Phase-sensitive ^{1}H-^{13}C DEPT-edited HSQC (right) and TOCSY{^{31}P} NMR spectra in $MeOD_4$.

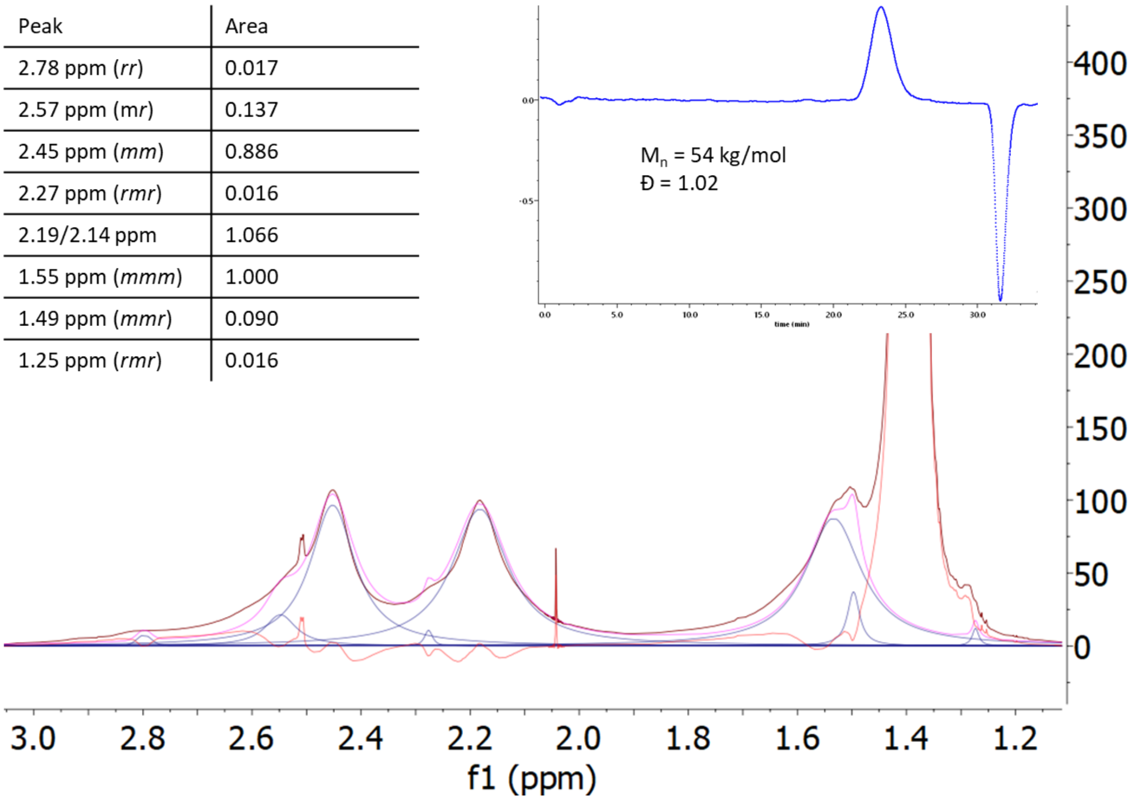

Peak	Area
2.78 ppm (*rr*)	0.017
2.57 ppm (mr)	0.137
2.45 ppm (*mm*)	0.886
2.27 ppm (*rmr*)	0.016
2.19/2.14 ppm	1.066
1.55 ppm (*mmm*)	1.000
1.49 ppm (*mmr*)	0.090
1.25 ppm (*rmr*)	0.016

Figure S25. Quantification of the *mmm* tetrads with the line fitting method of MestReNova version 14.0.0-23239 and the GPC trace. Color coding: dark red – original spectrum, blue – peaks, pink – sum, red – residue.

NMR spectra & GPC trace of Table 1, run 5:

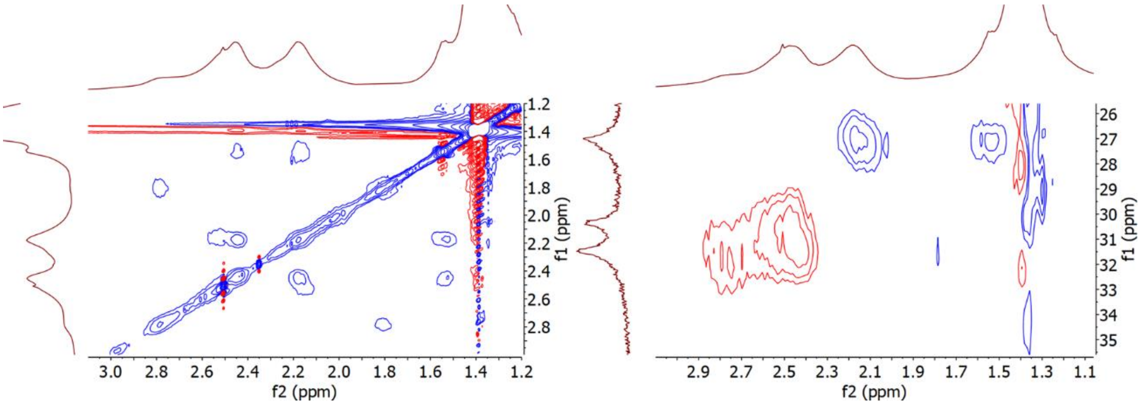

Figure S26. Phase-sensitive ^{1}H-^{13}C DEPT-edited HSQC (right) and TOCSY{^{31}P} NMR spectra in MeOD$_4$.

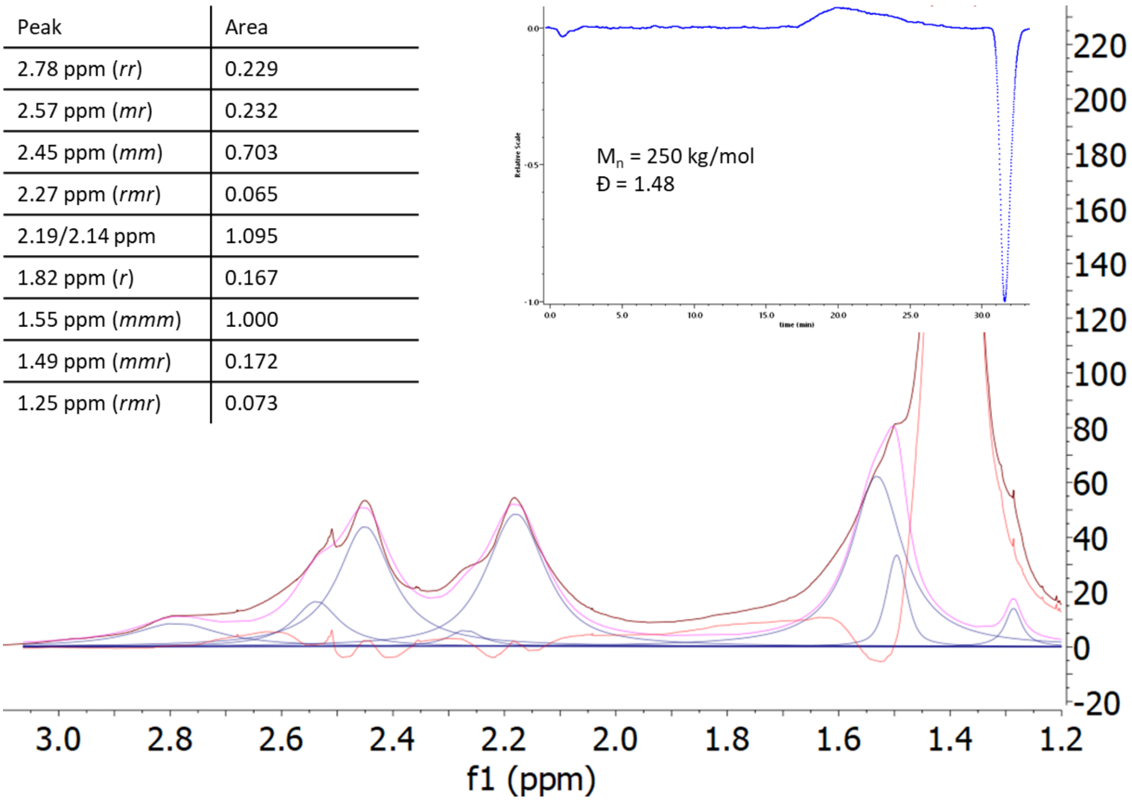

Peak	Area
2.78 ppm (*rr*)	0.229
2.57 ppm (*mr*)	0.232
2.45 ppm (*mm*)	0.703
2.27 ppm (*rmr*)	0.065
2.19/2.14 ppm	1.095
1.82 ppm (*r*)	0.167
1.55 ppm (*mmm*)	1.000
1.49 ppm (*mmr*)	0.172
1.25 ppm (*rmr*)	0.073

Figure S27. Quantification of the *mmm* tetrads with the line fitting method of MestReNova version 14.0.0-23239 and the GPC trace. Color coding: dark red – original spectrum, blue – peaks, pink – sum, red – residue.

NMR spectra & GPC trace of Table 1, run 7:

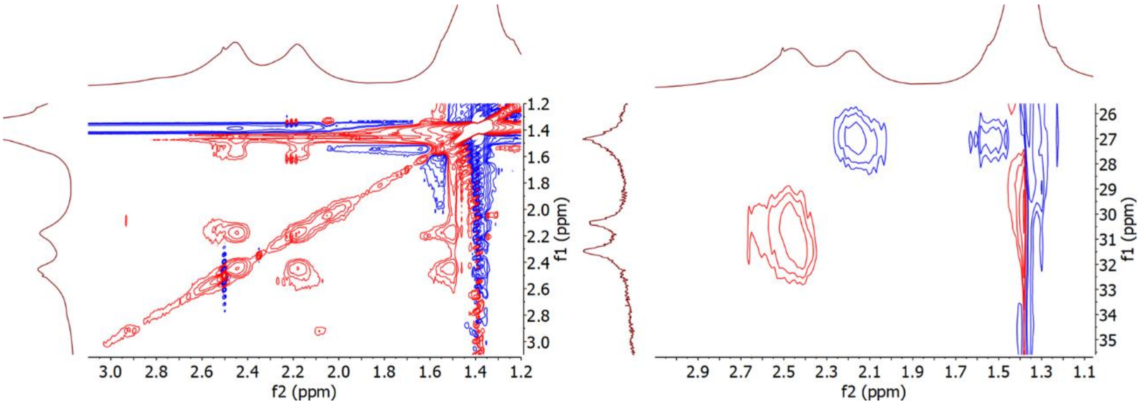

Figure S28. Phase-sensitive ^{1}H-^{13}C DEPT-edited HSQC (right) and TOCSY{^{31}P} NMR spectra in $MeOD_4$.

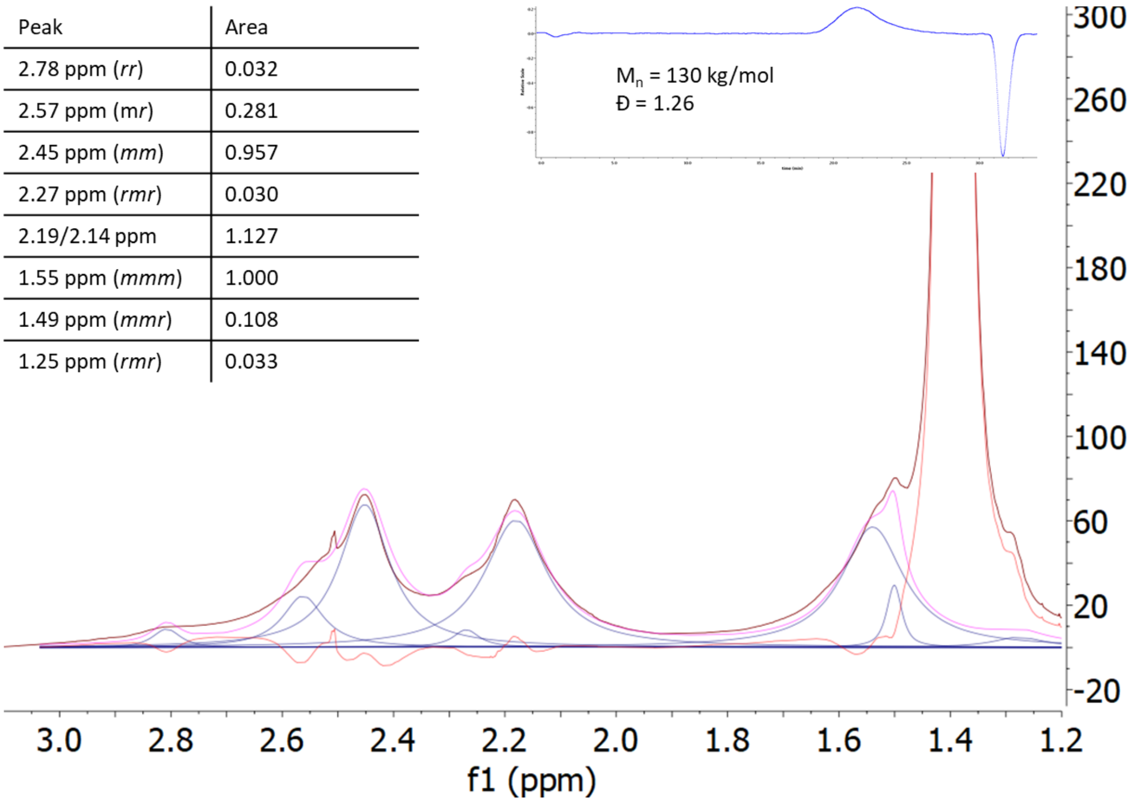

Peak	Area
2.78 ppm (*rr*)	0.032
2.57 ppm (m*r*)	0.281
2.45 ppm (*mm*)	0.957
2.27 ppm (*rmr*)	0.030
2.19/2.14 ppm	1.127
1.55 ppm (*mmm*)	1.000
1.49 ppm (*mmr*)	0.108
1.25 ppm (*rmr*)	0.033

Figure S29. Quantification of the *mmm* tetrads with the line fitting method of MestReNova version 14.0.0-23239 and the GPC trace. Color coding: dark red – original spectrum, blue – peaks, pink – sum, red – residue.

NMR spectra, thermal characteristics & GPC trace of Table 1, run 8 (polymer B):

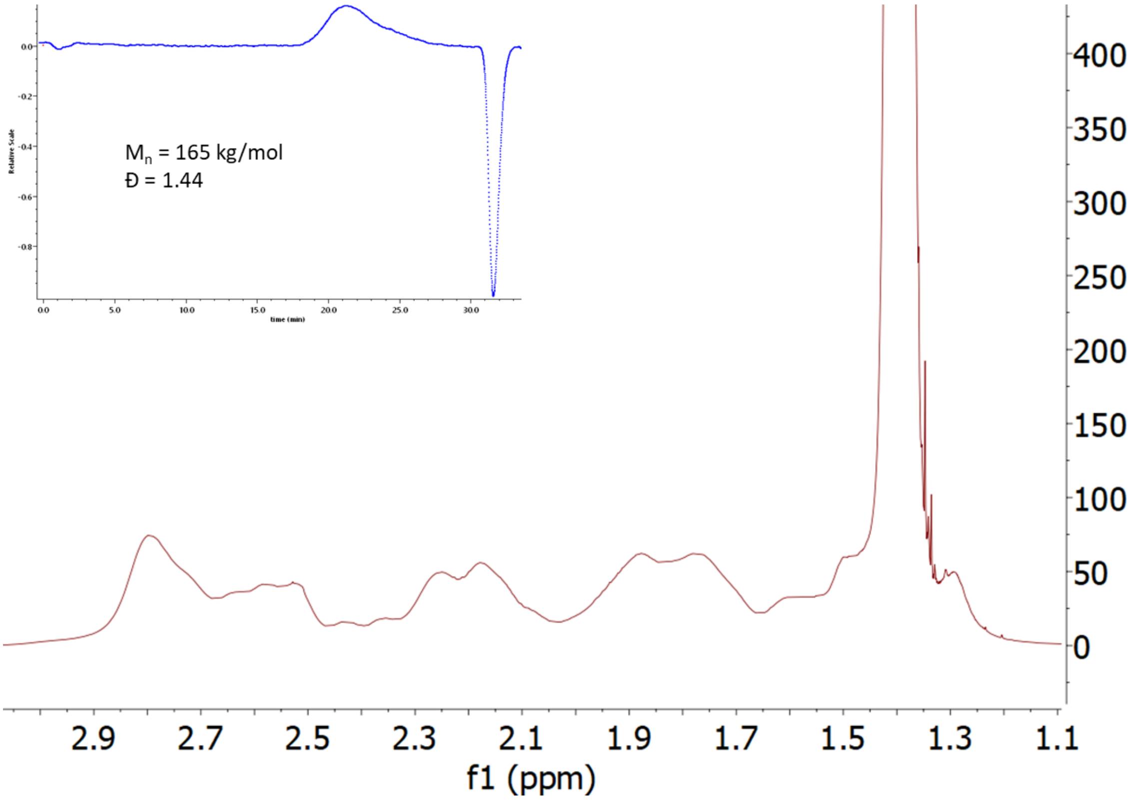

Figure S30. ^{1}H{^{31}P} NMR spectrum and the GPC trace.

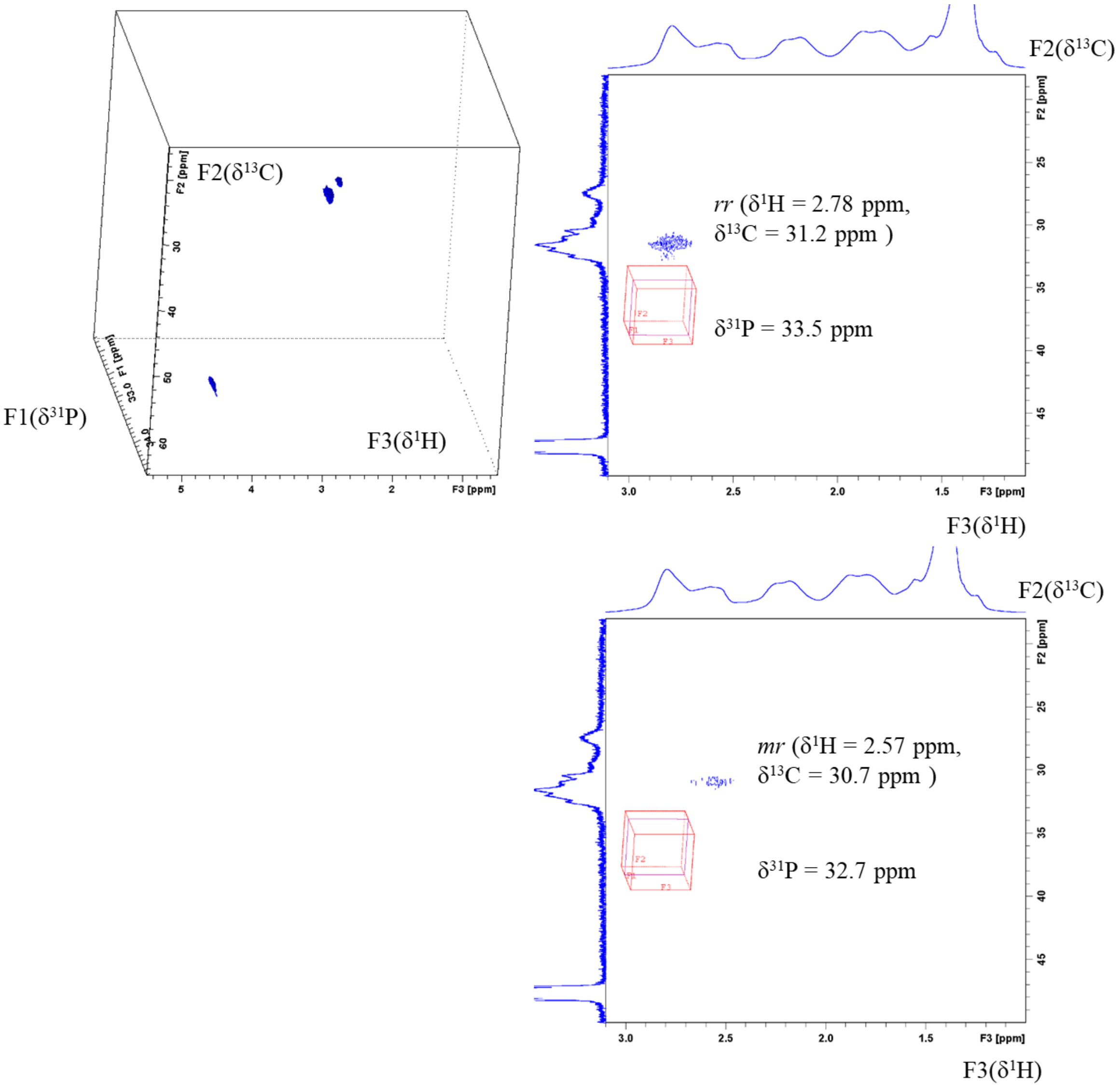

Figure S31. ^{1}H-^{13}C-^{31}P triple resonance HCP 3D experiment edited by J_{PC} = 110 Hz (for details see Table S11, S12).

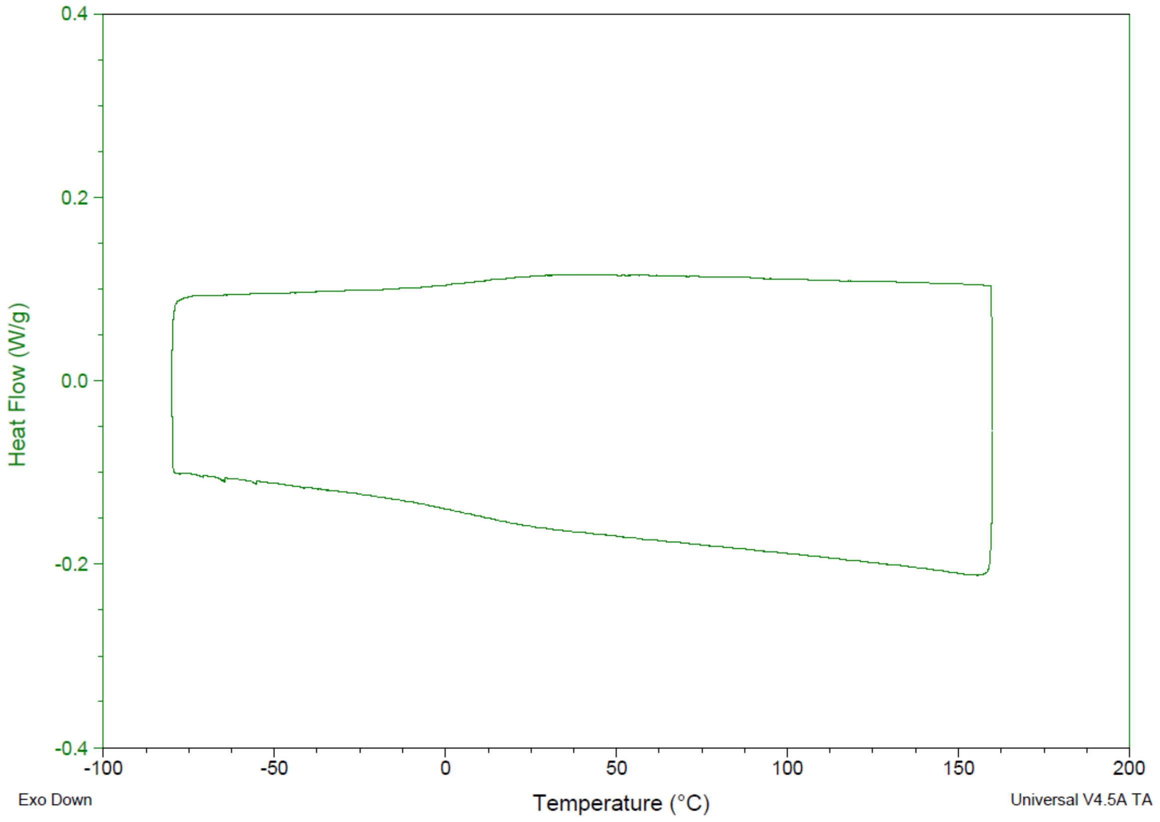

Figure S32. DSC analysis of polymer **A** showing no melting point.

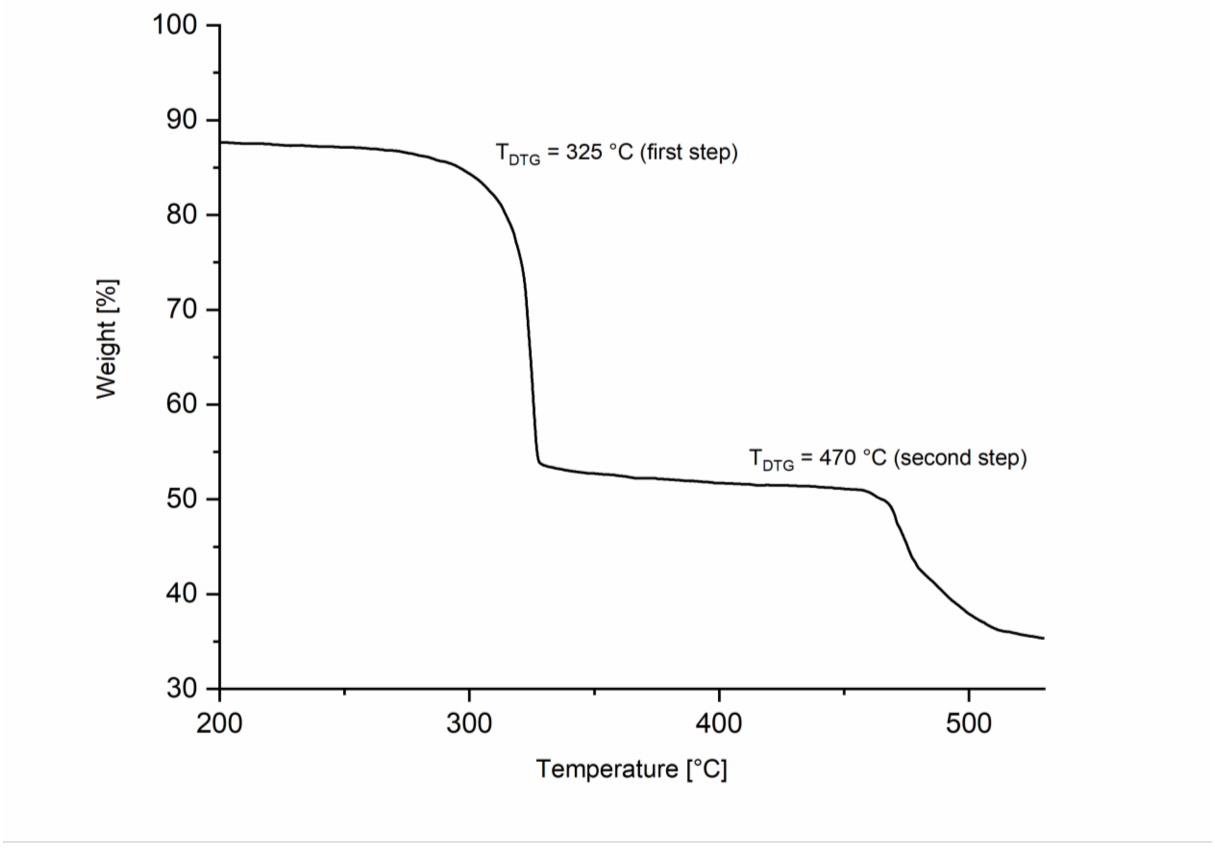

Figure S33. Thermogravimetric analysis of polymer **A**.

NMR spectra & GPC trace of Table 1, run 10:

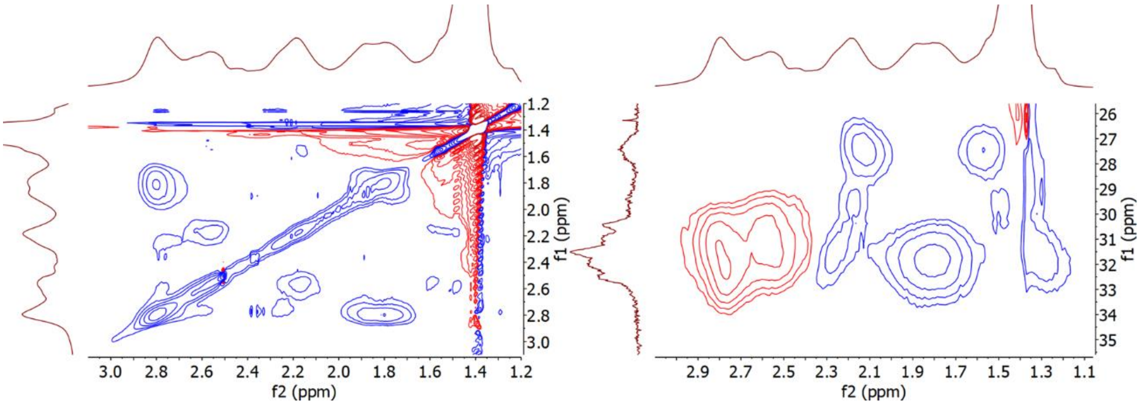

Figure S34. Phase-sensitive ^{1}H-^{13}C DEPT-edited HSQC (right) and TOCSY{^{31}P} NMR spectra in MeOD$_4$.

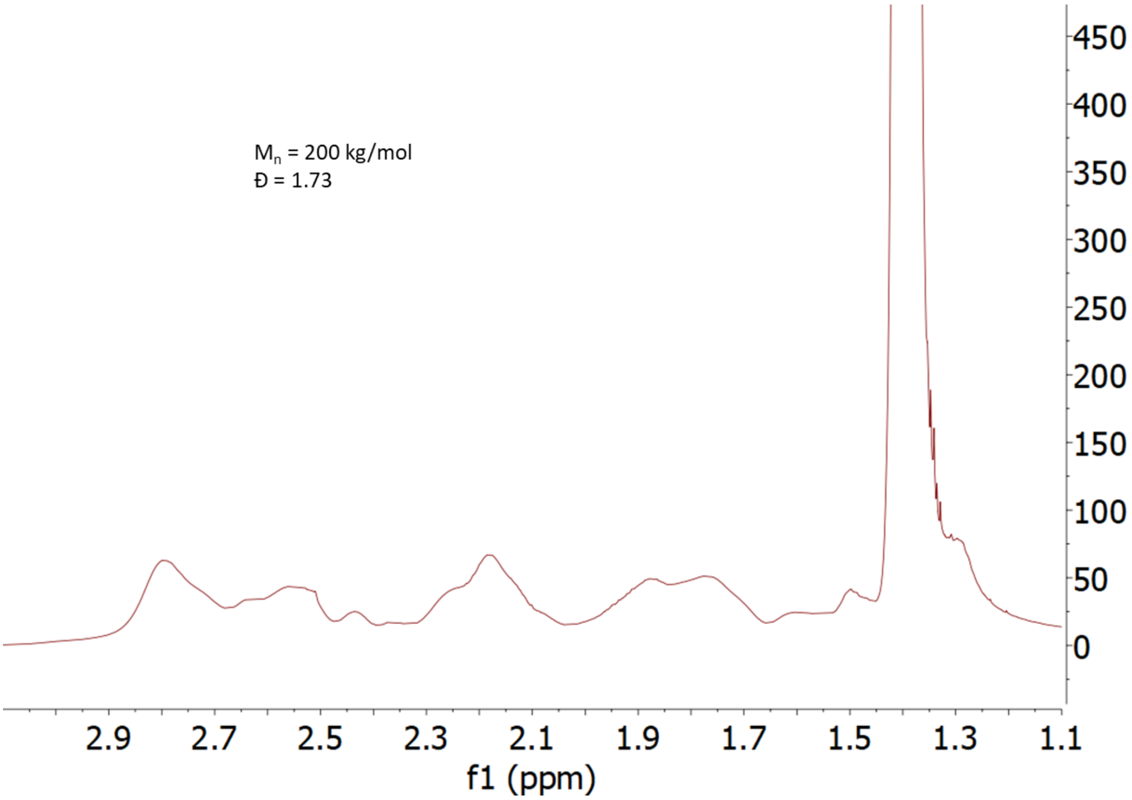

Figure S35. ^{1}H{^{31}P} NMR spectrum and the GPC trace.

Saponification of Table 1, run 4 (polymer B):

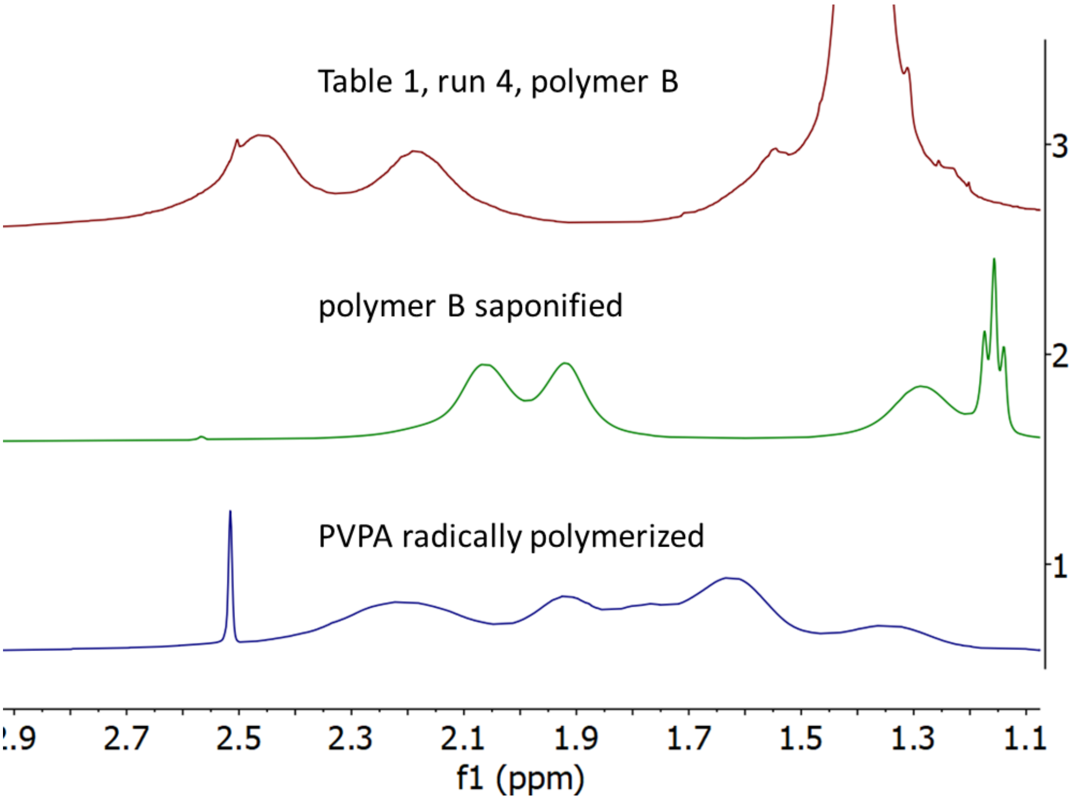

Figure S36. ^{1}H NMR spectra of polymer B in $MeOD_4$ and its saponification product in D_2O (1. 10 g/L DEVP in DCM + excess TMSBr 24 h reflux; 2. 1 m HCl 2 h r.t. and aqueous dialysis) compared to a radically produced PVPA in D_2O.

5. References

(1) Behr, A. *Angewandte homogene Katalyse*; Wiley-VCH Verlag GmbH & Co. KGaA: Weinheim, 2008.

(2) van Leusen, D.; Beetstra, D. J.; Hessen, B.; Teuben, J. H. Ethylene-Bridged Tetramethylcyclopentadienylamide Titanium Complexes: Ligand Synthesis and Olefin Polymerization Properties †. *Organometallics* **2000**, *19*, 4084–4089, DOI: 10.1021/om000402f.

(3) Resconi, L.; Camurati, I.; Grandini, C.; Rinaldi, M.; Mascellani, N.; Traverso, O. Indenyl-amido titanium and zirconium dimethyl complexes: improved synthesis and use in propylene polymerization. *J. Organomet. Chem.* **2002**, *664*, 5–26, DOI: 10.1016/S0022-328X(02)01853-3.

(4) Hou, Z.; Koizumi, T.-a.; Nishiura, M.; Wakatsuki, Y. Lanthanide(II) Complexes Bearing Linked Cyclopentadienyl−Anilido Ligands: Synthesis, Structures, and One-Electron-Transfer and Ethylene Polymerization Reactions. *Organometallics* **2001**, *20*, 3323–3328, DOI: 10.1021/om010261x.

(5) Carpenetti, D. W.; Kloppenburg, L.; Kupec, J. T.; Petersen, J. L. Application of Amine Elimination for the Efficient Preparation of Electrophilic ansa-Monocyclopentadienyl Group 4 Complexes Containing an Appended Amido Functionality. Structural Characterization of $[(C_5H_4)SiMe_2(N\text{-}t\text{-}Bu)]ZrCl_2(NMe_2H)$. *Organometallics* **1996**, *15*, 1572–1581, DOI: 10.1021/om950858a.

(6) Hultzsch, K. C.; Spaniol, T. P.; Okuda, J. Half-Sandwich Alkyl and Hydrido Complexes of Yttrium: Convenient Synthesis and Polymerization Catalysis of Polar Monomers. *Angew. Chem. Int. Ed.* **1999**, *38*, 227–230, DOI: 10.1002/(SICI)1521-3773(19990115)38:1/2<227:AID-ANIE227>3.0.CO;2-M.

(7) Hultzsch, K. C.; Voth, P.; Beckerle, K.; Spaniol, T. P.; Okuda, J. Single-Component Polymerization Catalysts for Ethylene and Styrene: Synthesis, Characterization, and Reactivity of Alkyl and Hydrido Yttrium Complexes Containing a Linked Amido−Cyclopentadienyl Ligand. *Organometallics* **2000**, *19*, 228–243, DOI: 10.1021/om990583p.